The Holocene history of George VI Ice Shelf, Antarctic Peninsula from clast-provenance analysis of epishelf lake sediments.

Roberts, S.J.[1*], Hodgson, D.A.[1], Bentley, M.J.[2, 1], Smith, J.A.[1, 2], Millar, I.L.[3], Olive, V.[4], Sugden, D. E.[5]

[1] British Antarctic Survey (BAS), Natural Environment Research Council (NERC), High Cross, Madingley Rd, Cambridge, CB3 0ET, UK.

[2] Department of Geography, University of Durham, South Rd, Durham, DH1 3LE, UK.

[3] NERC Isotope Geosciences Laboratory, British Geological Survey, Keyworth, Nottingham, NG12 5GG, UK.

[4] Scottish Universities Environmental Research Centre, Scottish Enterprise and Technology Park, Rankine Avenue, East Kilbride, G75 0QF, Scotland.

[5] School of GeoSciences, University of Edinburgh, West Mains Road, Edinburgh, EH9 3GW.

* Corresponding author

Keywords: Antarctica, lakes, isotope geochemistry, sedimentology, climate change, ice shelf

Word counts: Text = 9002

Abstract = 437

Abstract

The Antarctic Peninsula has experienced a dramatic increase in temperature and the loss of c. 14,000 km^2 of ice-shelf area in recent years. During this time George VI Ice Shelf (GVIIS) has remained relatively intact, but is now reaching its theoretical limit of viability. Epishelf lakes, formed when ice shelves dam the mouths of marine embayments, accumulate sediments that can be used to constrain past ice-shelf behaviour. They are stratified water bodies with an upper layer of fresh melt-water overlying a marine layer of water. Multi-proxy analysis of a sediment core from Moutonnée Lake, an epishelf lake dammed by GVIIS on the east coast of Alexander Island, has recently shown that it retreated to at least the Ablation Point area in the early Holocene, c. 9600-7500 yr BP, demonstrating its vulnerability to periods of atmospheric and oceanic warmth. This study tests this interpretation of ice-shelf collapse through detailed analyses of granulometric, geochemical and Sr and Nd isotope provenance data for >8 mm clasts from the same cores. Clast data from Moutonnée Lake were compared with geological reference data from two further lakes on Alexander Island (Ablation Lake and Citadel Bastion Lake) and an extensive archive of rocks and isotope geochemical provenance data from the Antarctic Peninsula region. Underpinning this provenance analysis is the contrast between the plutonic/igneous outcrops in Palmer Land on the western side and the predominantly sedimentary strata of Alexander Island on the eastern side of George VI Sound, and the different patterns in their deposition that would be expected at Moutonnée Lake during periods of ice shelf presence and absence. Results show that changes in clast distribution and provenance reflect the early Holocene retreat and reformation of George VI Ice Shelf at Moutonnée Lake. The period of ice shelf retreat was marked by the onset of marine conditions in the basin followed by a rapidly deposited zone of clasts whose provenance, distribution, varied lithology and larger than average clast size are indicative of a period of lake-ice disintegration and ice-rafted debris deposition between c. 9600-8450 yr BP. Igneous clasts in the ice-rafted debris have a close affinity with the plutonic provinces of western Palmer Land suggesting transport to the site by icebergs or recycling through Alexander Island strata/moraines. When epishelf lake conditions returned after c. 7500 yr BP, the clasts were smaller, the number of lithologies more limited and the assemblage dominated by olive-green vitric tuff and pale-green rhyolitic clasts that isotope data link to Early Cretaceous volcanic activity in Palmer Land. Their dominance in the upper part of the core most likely relates to increased erosion of Palmer Land ash/tuffs from volcanic outcrops on the floor of Moutonnée Valley and implies a downturn in climate after c. 7500 yr BP and the reformation of George VI Ice Shelf.

1. Introduction

Recent atmospheric warming across the Antarctic Peninsula (AP) region has been substantially greater than both the current global mean and the natural temperature variability of the Holocene (Scambos et al., 2000; Vaughan et al., 2003; Domack et al., 2005). As a result, substantial volumes of ice have been lost from unconfined ice shelves (Fig. 1) (King et al., 2004). This process has led to accelerated glacier flow into the ocean, which contributes to raising global sea-levels (De Angelis and Skvarca, 2003; Scambos et al., 2004). Assessing the past stability of ice shelves on the AP improves our understanding of how the remaining ice shelves will respond to continued warming of the region predicted by many climate models (Houghton, 2001; De Angelis and Skvarca, 2003; Shepherd et al., 2003).

George VI Ice Shelf (GVIIS) is the largest remaining ice shelf on the western side of the AP (Fig. 1). It is c. 500 km long, 20-60 km wide and 100-500 m thick and confined within George VI Sound (70^{o}-73^{o} S, 68^{o}-72^{o} W) by Alexander Island to the west and Palmer Land to the east. Unlike most Peninsula ice shelves that have recently disintegrated, its confinement provides additional stability (Smith et al., in press). On the eastern coast of Alexander Island, GVIIS impounds two epishelf lakes, Moutonnée and Ablation (Fig. 2). In Antarctica, epishelf lakes form when ice shelves dam marine embayments. Moutonnée Lake is a tidal, stratified water body with a lower marine layer that extends under the ice shelf to the ocean and an upper fresh melt-water layer whose maximum thickness is determined by the draught of the ice shelf (Heywood, 1977; Smith et al., 2006). Smith et al. (2006) proposed that when the ice-shelf is absent, Moutonnée Lake would become a marine embayment (Fig. 3). Therefore, epishelf lakes can be used to constrain past ice-shelf behaviour because when the ice-shelf retreats marine sediments with a distinctive biological and isotopic signature are deposited.

The recent loss of the Larsen Ice-shelf B (LIS-B) is unique in the present Holocene interglacial (Domack et al., 2005). However, other ice shelves are behaving, and have behaved differently with evidence for retreat events in the mid and early Holocene (Pudsey and Evans, 2001; Brachfeld et al., 2003; Bentley et al., 2005; Cook et al., 2005). For example, Bentley et al. (2005) and Smith et al. (2006) showed that GVIIS retreated to at least the Ablation Point area in the early Holocene, c. 9595-7495 yr BP, immediately post-dating the early Holocene climatic optimum identified in ice core records (Masson et al., 2000; Masson-Delmotte et al., 2004), and occurring at the same time as an influx of warmer ocean water onto the AP continental shelf (Domack et al., 2001; Bentley et al., 2005; Smith et al., 2006). It is thought that structural instability and collapse of unconfined ice shelves such as Larsen Ice Shelf B and C followed a build up of superficial meltwater ponding, with increased lateral stress leading to rapid removal of large sections of the ice shelf (Doake et al., 1998). In contrast, superficial ponding has been observed for decades on GVIIS, and although regional temperatures have risen to its hypothesised viability limit, it has remained relatively stable with only minor retreat

recorded at its northern margin since 1985 (Fig. 4) (Vaughan and Doake, 1996). Thus, a combination of oceanic melting of the under-side of the ice shelf and increases in atmospheric temperature at the surface may be necessary for further retreat of GVIIS beyond present day limits (Shepherd et al., 2003; Bentley et al., 2005; Smith et al., 2006).

The aim of this study is to examine the geological evidence for past retreat of GVIIS through detailed analyses of granulometric, geochemical and Sr and Nd isotope provenance data for clasts retained on an 8 mm sieve (i.e. the >8 mm fraction) in a sediment core from Moutonnée Lake. We compare data from Moutonnée Lake with geological reference data from two other lakes on the eastern side of Alexander Island, Ablation Lake and Citadel Bastion Lake, and an extensive archive of rocks and geological provenance reference data from the AP region. Specific objectives are to determine if the granulometric and geochemical characteristics of the clasts can be used: (1) as an indicator of initial and/or final provenance, (2) as a proxy record for GVIIS collapse and/or reformation and (3) as an indicator of major changes in glacial activity in the lake-catchment.

Underpinning this provenance analysis is the contrast between the plutonic/igneous outcrops in Palmer Land on the western side of George VI Sound and the predominantly sedimentary strata of Alexander Island on the eastern side of George VI Sound, and the different patterns in their deposition that would be expected at Moutonnée Lake during periods of ice shelf presence versus periods of ice-shelf absence. At present, locally derived clasts enter Moutonnée Lake mainly by glacial erosion of catchment bedrock or moraines, and possibly even aeolian transport (cf. Lewis et al., 2002; Gilbert and Domack, 2003). A smaller number of exotic clasts are also transported englacially through GVIIS from Palmer Land and become embedded in the lake ice margin or deposited via a local lake ice conveyor along the lake shoreline (Clapperton and Sugden, 1982; Potter and Paren, 1985; Hendy, 2000; Bentley et al., 2005; Smith et al., in press). When the ice-shelf was absent in the early Holocene, the lake would have become a marine embayment. The main conclusion from this study is that during this period of ice-shelf absence a greater number of exotic clasts were deposited in the embayment by lake-ice disintegration and iceberg rafting processes.

2. Site descriptions

2.1 Moutonnée Lake

Moutonnée Lake (70^{o} 52.123' S, 68^{o} 19.635' W) is an epishelf lake impounded by GVIIS and located in a valley on the east coast of Alexander Island (Fig. 2a). The geology and geomorphology of the area are well-mapped, with catchment glaciers currently located c. 2 km up the valley (Fig. 2) (e.g., Horne, 1968; Elliott, 1975; Clapperton and Sugden, 1983; Butterworth, 1991; Browne, 1996). At Moutonnée Lake, GVIIS is grounded on a partially submerged bedrock bar damming the embayment (Figs. 2b, 3). However the lake retains a limited hydraulic connection to the seawater in George

VI Sound as revealed by the offset tidal regime that occurs in the lake (Pearson and Rose, 1983). At present, freshwater overlies seawater with a halocline at c. 30 m depth (Heywood, 1977; Smith et al., 2006). We examined the principal core, ML, extracted from the deepest point of the main basin with a water depth of 51 m.

A conceptual model has shown that when the ice shelf is present exotic clasts can be transported across George VI Sound from the igneous provinces of western Palmer Land by becoming incorporated into the ice-shelf and then the lake ice (Fig. 3) (Smith et al., 2006). Bishop and Walton (1981) and Pearson and Rose (1983) demonstrated the existence of a strong south-east to north-west flow regime from the region south of the Bertram Glacier in western Palmer Land in the direction of Ablation Point (Fig. 4). Clapperton and Sugden (1982) and Smith et al. (2006) also noted the presence of granitic clasts in the moat surrounding Moutonnée Lake, showing that transport of material across GVIIS had occurred at some point, likely due to the existence of a lake-ice conveyor similar to that described in Hendy (2000). The ice-shelf at both Moutonnée Lake and Ablation Lake (AB) is not continuously grounded. Processes similar to those occurring at Moutonnée Lake are likely to have occurred at Ablation Lake.

2.2 Reference data sets

Ablation Lake and Citadel Bastion Lake

Ablation Lake (70^{o} 48.974' S, 68^{o} 27.143 W) has a similar setting to Moutonnée, but differs in that GVIIS is only partially grounded across the entrance to the embayment. This results in a continuous hydraulic connection to the seawater in George VI sound as revealed by an in-phase tidal regime occurring in the lake (Smith et al., in press). Due to the absence of a bedrock barrier GVIIS penetrates into the basin forming an ice-shelf tongue (Fig. 2b: H) and can directly deposit coarse sediments into the lake. We examined the principal Ablation Lake core, henceforth referred to as AB, extracted from a water depth of 65 m.

Citadel Bastion Lake (72° 00.549’ S, 068° 27.708’ W) (Fig 1) is located on the eastern side of Alexander Island, south of and further inland than Moutonnée and Ablation Lakes. It is enclosed on three sides by Citadel Bastion and Corner Cliffs and dammed along its northern edge by the Saturn Glacier (Fig. 2c, d), which isolates it from George VI Sound. Therefore, it provides useful reference data for modes and types of local clast deposition that would be expected on Alexander Island at a site beyond the influence of the ice-shelf. There is no subglacial hydraulic connection to George VI Sound and the Saturn Glacier prevents seawater encroaching into the embayment. We examined the principal core (CIB) extracted from a water depth of 89 m.

2.3 Geological reference data

To best interpret the provenance signals of clasts identified in the ML, AB and CIB cores, we examined previously collected rocks and geological data from across Alexander Island and western Palmer Land. The AP is composed of Late Jurassic to Early Cretaceous calc-alkaline igneous rocks and fore-arc and back-arc volcaniclastic sedimentary sequences. The latter were formed by subduction of the Pacific and proto-Pacific beneath the AP along an active continental margin of Gondwana (Suarez, 1976; Saunders et al., 1980; Pankhurst, 1982; Pankhurst, 1990; Leat et al., 1995; Howe, 2003). Vaughan and Storey (2000) proposed a terrane model to explain the formation and geology of the AP and the distinct geological contrast that exists between the predominantly volcanic and plutonic bedrock of western Palmer Land and the sedimentary deposits of eastern Alexander Island (Fig. 4). The three principal terranes are: (1) the Western Domain, an accretionary, predominantly sedimentary terrane covering Alexander Island, (2) the Central Domain, a magmatic subduction-related arc terrane exposed along the west coast of Palmer Land dominated by plutonic and volcanic outcrops and (3) the Eastern Domain, a cratonic margin terrane covering the east coast of Palmer Land, not relevant to this study. The Western Domain of Alexander Island is separated from the Central and Eastern Domains by a rift zone that runs the length of George VI Sound (Pearson and Rose, 1983; Bell and King, 1998).

The plutonic and volcanic provinces of western Palmer Land and southern Graham Land were formed by magmatic activity during the Mesozoic (Suarez, 1976; Leat et al., 1995; Storey et al., 1996; Howe, 2003). The Western Domain of Alexander Island formed in a fore-arc basin setting and is either a subduction/accretion complex of the Central Domain or a separate crustal fragment (Elliott, 1974; Vaughan and Storey, 2000). The bedrock in the catchment areas of the three lakes examined belongs to the Himalia Ridge Formation (Fig. 2b), part of the Fossil Bluff Group (FBG). The FBG is a fore arc sedimentary sequence, deposited during the Late Jurassic-Late Albian (c. 100 Ma) and outcropping along the eastern coast of Alexander Island (Macdonald et al., 1993; Moncrieff and Kelly, 1993). It is predominantly sedimentary, and characterised by interbedded black mudstones/siltstone, conglomerate, sedimentary breccia and arkosic sandstone strata (Doubleday et al., 1993; Macdonald et al., 1993; Moncrieff and Kelly, 1993; Miller and Macdonald, 2004). The Himalia Ridge Formation, which outcrops around the Ablation Point area, is a 1100 m thick sequence dominated by mudstone and sporadic conglomerate beds (Doubleday et al., 1993; Doubleday, 1994). Thick fluvial and deltaic sequences and interspersed volcanic deposits are exposed in and around the catchments of the three lakes examined. These were deposited unconformably during the Cretaceous on older metasediments of the Lemay Group and later uplifted, compressed and inverted during a mid-Cretaceous compression event. The FBG is largely devoid of igneous strata because volcanic activity migrated northwards, away from the Fossil Bluff area (McCarron and Millar, 1997; Howe, 2003).

3. Experimental Methods

3.1 Rationale

In marine core studies, granulometric investigations are commonly undertaken on the >2 and/or <2 mm fractions that define the boundary between sand and gravel (e.g., Pudsey et al., 1994; Pudsey, 2000; O Cofaigh et al., 2001; Pudsey and Evans, 2001; Anderson et al., 2002). The assumption that the >2 mm fraction is primarily ice-rafted debris (IRD) is valid in these studies because marine cores are often extracted far enough from terrestrial inputs to rule out other depositional mechanisms (Andrews and Principato, 2002).

In this study, the >2mm fraction was subdivided into 2-8 mm and >8 mm fractions because:

(i) Research on modern lacustrine environments in Antarctica suggests that coarse sand, fine gravel and coarser sediments are commonly found embedded in floating lake ice, while silts and fine sands rain-out onto the lake floor after melting through the ice. For example, Hendy (2000) noted that clasts <10 mm in thickness will pass through the lake ice and rain out because the rate at which they absorb and retain radiation, and, therefore, the rate at which they melt through the lake ice, is greater than the ablation rate of the lake-ice surface. That is, most individual clasts and clast aggregates >8 mm will remain embedded in the lake-ice. Since few clasts of this size melt through the ice before break-up, increased concentrations of clasts >8 mm in size and/or changes in their lithology in the lake sediment should represent periods when lake ice break-up and ice-rafting events occur.

(ii) Catchment glaciers probably calved periodically into the lakes (Clapperton and Sugden, 1982), allowing numerous 2-8 mm and >8 mm clasts to be transported into the lake by glacial and/or glaciofluvial processes. At Ablation Lake and Citadel Bastion Lake, catchment glaciers feed directly into the lake (Fig. 2b and 2c). In contrast, at Moutonnée Lake there are no direct inputs from the glaciers in Moutonnée Valley (Clapperton and Sugden, 1983) and any increase in >8 mm clast abundance and change in lithology would be most likely due to lake ice break-up and/or ice rafting.

(iii) >8 mm clasts can be readily classified into specific lithological groups whose granulometric and geochemical characteristics are more diagnostic of transport mechanisms and provenance than finer fractions.

(v) The >8 mm fraction is sufficiently abundant in all three cores for statistical analysis and clasts in this fraction provide sufficient material for standard analytical procedures (e.g., XRF, ICP-MS).

3.1 Core extraction, clast separation and chronology

Cores were extracted using a UWITEC gravity corer (for surface sediments) and a 2 m UWITEC KOL ‘Kolbenlot’ cable-operated percussion piston corer (for deeper sediments) and transported frozen to the UK. Following a series of routine descriptions and sedimentological analyses, sub-samples from each 1 cm of the cores were dried, weighed, re-suspended

in water, placed in an ultrasound bath for 45 minutes and wet sieved through 8 mm, 2 mm and 63 μm meshes. This paper concentrates on the >8 mm fraction. Detailed results of other sedimentological analyses including biological analyses of foraminifera, diatoms, geochemical and isotopic ($\delta^{18}O$, $\delta^{13}C_{org}$, TOC, NOC, C/N) and physical analyses (magnetic susceptibility) are described in Bentley et al. (2005) and Smith et al. (2006).

Clasts retained on the 8 mm sieve were grouped into lithological types on the basis of hand specimens and the representative geochemical and isotopic analyses. In total, more than 1000 clasts were grouped, weighed, and their long, intermediate and short axes measured. The number of clasts examined from each lake is approximately three times greater than the number of gravel clasts examined in comparable studies (e.g., Kuhn et al., 1993). Similarly, many of the lithological group and core zone divisions contain more than the 117 grains recommended for reliable statistical analysis in single-grain geochronology/provenance studies (Vermeesch, 2004).

Following recommendations in similar studies (Jones et al., 2000; Hodgson et al., 2004), monospecific marine foraminifera (*Globocassidulina* sp. and *Cibicides* sp.) and other macrofossils (e.g., plant remains and organic matter) were handpicked, cleaned and radiocarbon dated (see Table 1 for full experimental details). When macrofossils were absent, bulk surface sediments were dated on an exploratory basis to test the suitability of bulk sediment dating elsewhere in core (Table 1). Radiocarbon ages from marine organisms were calibrated to a calendar time scale using CALIB v4.4 (Stuiver and Reimer, 1993) and a ΔR value of 900 yr (Table 1).

3.2 Geochemical and isotopic analysis

Major, trace and Nd and Sr isotope analyses were undertaken on 35 representative clast types from the Moutonnée Lake core (ML) and the Ablation (AB) Lake core. At the outset, major and trace element and isotope data were thought to be good provenance indicators because of the macroscale differences in geology between Palmer Land and Alexander Island. Criteria for sampling were: (1) best representation of lithological diversity, (2) lack of significant visible alteration, and (3) suitable size of clast. Most of the clasts analysed come from the ML core, reflecting the greater diversity of clast types found in this core. Thin sections were made from all clasts prior to chemical analysis. For geochemical and isotope analysis, the outer/weathered surfaces were removed by grinding, the remaining sample crushed in a mini-rock splitter and ground by hand to a fine powder in a clean agate pestle and mortar. All crushing/grinding equipment was rigorously cleaned between samples with acetone in an ultrasonic bath. Geochemical procedures are summarised in relevant table captions.

It was not possible to date the clasts directly due to their limited size and/or lack of suitable or sufficient phenocrysts. Clast age estimates used in εNd calculations were obtained from isochron analysis of bulk $^{87}Sr/^{86}Sr$ vs $^{87}Rb/^{86}Sr$ data, which was analysed using Isoplot (Ludwig, 2003). εNd_i values, representing the difference between the initial $^{143}Nd/^{144}Nd$ ratio of the clasts and that of the chondritic uniform reservoir (CHUR) at the time of clast formation, were calculated using age estimates from $^{87}Sr/^{86}Sr$ vs $^{87}Rb/^{86}Sr$ isochron analysis and compared with Palmer Land datasets of known age. Initial hand specimen groupings were improved by agglomerative hierarchical cluster analysis of selected REE and isotopic data. Multivariate statistical analyses were used to compare new data with published Sr and Nd isotope data from Palmer Land. To aid interpretation of clast data, additional geochemical and isotope analysis was undertaken on the potentially far-travelled clay/silt (<63 μm) sediment fraction from the ML core. Eighteen powdered samples were subjected to the same geochemical/isotope procedures as the clasts.

4. Stratigraphic results

4.1 Core descriptions, stratigraphic units and chronology

The sediment matrix in the ML core is uniformly light grey (2.5Y 3/2-5/2, 5YR 4/1 and 10YR 3/1) with no major visible variations. A similar matrix was found in AB and CIB cores. The principal sedimentary facies in ML and AB are unstratified matrix- and clast-supported diamictons, fine mud with sporadic clasts, and sandy gravels. Clast-supported diamictons are more prevalent in the AB core than the ML or CIB cores and are more common in the bottom half of the AB and ML cores. The upper 30 cm of Zone 4 and the near surface 15-20 cm of all cores are dropstone muds/fine muds. Macrofossils were only found in the ML cores.

ML core: The ML core is divided into five principal units defined by the presence/absence of marine organisms (Fig. 5). Zone 1 is devoid of macro- and microfossils. Above this, Zone 2 (522-490 cm) is well defined by the appearance of marine organisms (forams, diatoms, spicules and brachipod shell fragments). Zone 3 is devoid of biogenic organisms, but characterised by a greater-than-average number of randomly deposited clasts of various sizes and rock type. Organisms indicative of marine conditions reappear in Zone 4 (302-236 cm). In the uppermost unit if the core, Zone 5 (236-0 cm), marine fossils are replaced by sporadic terrestrial organic matter and sparse moss fragments.

AMS ^{14}C ages from discrete macrofossils (mono-specific forams) in the ML core are in stratigraphic order (within 2σ error). Calibrated AMS ^{14}C foram ages from top of Zone 2 (9400±40 and 9260±110 cal yr. B.P.) and the lower half of Zone 4 (9400±30; 9470±30; 9430±40 cal. yr. B.P.) are essentially coeval (Table 1; Fig. 5). This means that the clast-dominated Zones 2 & 3 and the lower half of Zone 4 were deposited rapidly, with Zones 2 and 3 deposited not long after

the onset of marine conditions. Zone 5 remains undated due to insufficient macrofossils and problems with 'old' radiocarbon ages from bulk sediments. Exploratory radiocarbon dating of bulk surface sediments from the ML core produced a clearly erroneous age of 15100±50 ^{14}C yr BP (Table 1). This substantial age offset is comparable in magnitude with surface ages from other cores we have examined in this region (Table 1), and most likely due to sources of 'old' particulate organic carbon (POC) (e.g., lignite) present in the Fossil Bluff Group and/or old carbon from glacial meltwater (cf. Doran et al., 1999; Hendy and Hall, 2006). For these reasons we do not use bulk sediment ^{14}C ages in constructing chronologies for lake sediments from Alexander Island.

AB core: The reference core, AB was subdivided into five principal lithofacies units (Fig. 5) using criteria in Evans and Pudsey (2002). The core consists of a matrix-supported diamicton (Unit I), gravelly mud and muddy gravels with interbedded diamicton layers (Unit II), dropstone sandy mud and gravel (Unit III) and a matrix-supported diamicton (Unit IV) fining upwards into a virtually dropstone-free sandy mud near the surface (Unit V). An impenetrable deposit at c. 2.4 m prevented deeper coring, and, as a (likely) consequence, there is no evidence of the marine zones found in the longer ML core. The absence of macro- and microfossils or extractable organic fractions and compounds prevented reliable dating of the AB core. Humin and bulk sediment ages from this core are considered unreliable due to the likelihood of contamination from POC in the Fossil Bluff Group and/or old carbon in glacial meltwater (Table 1).

CIB core: The reference core, CIB consists of a silty-sandy mud with repetitious gravel deposits. It has been divided into five units (A-E) defined by the principal changes in physical characteristics (grain size and magnetic susceptibility) and organic content. Some bulk and humin radiocarbon ages are stratigraphically consistent, but the 'old' bulk surface ages suggest that contamination from old carbon sources also occurs at this site. Studies to refine this chronology using optically stimulated luminescence and palaeomagnetic intensity dating methods are ongoing. Until then, we assume that the core post-dates the Last Glacial Maximum (LGM) because the Citadel Bastion area was most likely inundated by ice at the LGM.

4.2 Clast distribution, density, shape and weathering characteristics

In the ML core, the mean clast mass of Zone 1 (62.8±57.4 g) is significantly larger than that of the other zones (Fig. 5). There are, however, only four clasts in this zone and all statistics are heavily skewed by sandstone bedrock embedded in the base of the core. Zone 2 (39 clasts; mean clast mass=18.9±7.6 g, clast density 0.458 g cm^{-3} sediment) and the first 10 cm of Zone 3 (31; 8.92±5.73 g; 0.229 g cm^{-3}) have mean clast masses and densities that are significantly greater than elsewhere in the ML core (and both AB and CIB cores) (Fig. 5). Zone 3 has largest number of clasts per cm in the ML

core (1.53), consistent with rapid deposition suggested by the radiocarbon results. More significantly, these data show that the largest clasts were deposited at the start of the marine incursion (Zone 2). Clast density and mean clast mass in Zone 4 is significantly less than in other zones (0.026 g cm^{-3}/3.05±0.88 g respectively, cf. mean of 0.110 g cm^{-3}/5.73 ±0.87 g) suggesting a lower rate of deposition throughout Zone 4. A further reduction in clast density to 0.0151 g cm^{-3} of sediment between 268-236 cm suggests IRD deposition ceased approximately half way through this zone. Interestingly, the top 17 cm of Zone 5 is similarly devoid of clasts. Indeed, the most notable similarity across all three cores is the near complete absence of clasts from the upper 15-20 cm. This could relate to a more recent reduction in clasts deposited from catchment glaciers that have receded beyond the lake margins (Figs. 2, 5).

The clast assemblage in ML differs from that in AB and CIB in several ways. First, the AB core has the greatest mean clast density (0.1921 g cm^{-3}) and mean clast mass (6.12±0.58 g). The overall mean clast mass of the ML core is similar to the AB core, but the clast density is significantly less, due to the lack of larger clasts (defined here as clasts >10 g) between 236-0 cm depth (Fig. 5). In contrast, the smaller proportion of glacially remoulded and striated clasts in the ML core of 8 % compared to 31% in the AB core indicates that input of material from a subglacial or entrained glacial source (e.g. basal ice-shelf transportation) is more limited in the ML core. The greater proportion of striated mudstone and siltstone (Group 14) clasts in the AB core most likely reflects the larger size and higher number of active glaciers present in Ablation Valley compared with the Moutonnée Valley (Fig. 2b). Third, as might be expected, the AB core is dominated by clasts from proximal catchment glaciers and direct inputs from the ice shelf tongue that protrudes into the lake. Fourth, due to its isolation from GVIIS, the mean clast density of the CIB core (0.0213 g cm^{-3}) is an order of magnitude smaller than the AB and ML cores. This is primarily because the clasts are smaller (Fig. 5), but there is also a marked reduction in the number of clasts per cm (ML=0.960, AB=1.580, CIB=0.75 clasts per cm) and clast density (ML=0.110 g cm^{-3}, AB=0.192 g cm^{-3}, CIB=0.0213 g cm^{-3}). The overall mean clast mass in CIB is 1.43±0.34 g (cf. ML=5.73±0.87 g, AB=6.12±0.58 g) and only five clasts have a mass greater than 10 g. Zone D is the only zone with a clast density >0.1 g cm^{-3} This zone is characterized by variable inputs of coarse/fine sediments that are thought to reflect fluctuations in the position of the calving front of the catchment glaciers.

Clast shape and weathering characteristics in the ML core differ from the AB and CIB cores. Clasts in the ML core are angular to sub-angular (mean shape=1.8±0.1; scale=0-6 where 0=very angular and 6=well-rounded) (Pettijohn et al., 1987), i.e. less well rounded than the average clast from AB (2.5±0.1) and CIB (2.6±0.1) cores. This is because the first 25 cm of Zone 3 has a large number of angular clasts, possibly representing clasts that were embedded in lake ice and dumped into the lake at the first opportunity with little or no recycling/reworking through Alexander Island moraines. The

higher degree of angularity in Zone 5 is due to the large number of very angular/angular olive green vitric tuff (Group 1) clasts (n=124; mean shape=1.2±0.1). Clasts in AB and CIB are sub-angular to sub-rounded and have a roundness index greater than average (2.5±0.1 and 2.6±0.04, respectively), possibly indicative of proportionately greater reworking or erosion from previously reworked deposits in the catchment strata (e.g. Fossil Bluff Group conglomerates).

Overall, the proportion of potentially subglacially/ice shelf entrained, derived and/or remoulded clast shapes (i.e. bladed or prolate clasts) remains fairly constant at 40-60% for all three cores and zones within the ML core. Clast shapes that might represent significantly longer periods of basal entrainment, or perhaps through ice-shelf transport commonly constitute 20-40%, with the largest percentage in all cores in marine Zone 4 of the ML core. There are more bladed clasts in the CIB core compared to the overall mean shape and the mean shapes for each core (CIB=21% vs ML=13%, AB=16%, All cores=16%). This is indicative, perhaps, of greater deposition of sediment entrained in the basal layers of catchment glaciers.

In the ML core 29% of mudstone clasts have multi-directional striations, suggesting multiple phases of glacial reworking before final deposition into the lake. The number of striated clasts is greatest in the AB core (31%) reflecting the dominance of Group 10/14 mudstones/siltstones (61% of all clasts) on which striations are more readily visible. Nevertheless, a greater than average number of Group 10/14 clasts are striated in the AB core (44% in AB compared 33% overall, 28 % in ML and 18% in CIB) (Table 2). The most significant pattern in the iron-oxide weathering statistics (Table 2) is that only 1% of clasts in the CIB core have visible iron-oxide weathering, far fewer than the ML and AB cores.

4.3 Lithological groups and key changes in their distribution

Thirty-five clast groups were identified in the three sediment cores with significant lithological and distributional differences between them (Fig. 6; Table 2). To aid descriptions of provenance, we have presented clast data in three main categories: primary igneous (plutonic and volcanic clasts), secondary igneous (volcanic clasts only) and non-igneous (sedimentary/meta-sedimentary clasts) (Table 2). Primary igneous clasts are defined by >50% crystalline or tuffaceous composition. Tuffs in this category contain <10% lithic fragments. Secondary igneous clasts are lithic tuffs or tuffaceous sandstones with >50% reworked lithic component. Non-igneous clasts are sedimentary and/or metamorphosed/reworked sedimentary clasts. These are dominated by black mudstones, and dark grey and grey-white sandstones commonly found in the bedrock strata of the Fossil Bluff Group.

There are 31 lithological groups represented in the ML core, with a maximum of 11 in any single 10 cm interval. The proportion of igneous and sedimentary clasts is almost equal when averaged over the whole core (50% and 45%, respectively). The number of plutonic clasts is c. 3-5% throughout, perhaps indicating input from a constant, but restricted source. However, general statistics mask significant differences in the distribution of clast types in the marine (Zones 2-4) and epishelf lake sediments (Zone 5). The majority of the clasts in marine zones (2 and 4) and in the marine IRD Zone 3 are sedimentary or meta-sedimentary. ML Zone 3 has the largest number of clast types (17 in total). The volcanic clast component of >30% in Zones 2 and 3, rises significantly to >80% in Zone 5.

There are three main shifts in clast distribution (Fig. 6: circled points 1-3). The most important of these is the shift in clast lithologies between Zones 3 and 5 (Fig. 6: circled points 1-2). In Zone 3, the clast assemblage is a mixture of fresh to highly weathered crystal and lithic tuffs and sedimentary clasts. Zone 4 comprises a dropstone mud deposit with a low proportion of volcanic clasts (21% volcanic clasts compared to a core average of 50%). The clast assemblage in epishelf lake sediments of Zone 5 is dominated (63%) by Group 1/7 fresh olive green vitric tuff clasts until c. 60 cm depth when they, and all other igneous deposits, disappear abruptly (Fig. 6). There is also a significant shift in the type of rhyolitic clasts deposited in Zone 3 compared to Zone 5. Group 2 green rhyolites, 89% of which are found in Zones 3 and 4, are replaced by Group 3 light green rhyolites, 88% of which are found in Zone 5. This change occurs at the same point in the core as the increased abundance of Group 1/7 clasts. As with Group 1/7 clasts, Group 3 rhyolites dominate the rhyolitic clast assemblage until c. 60 cm depth when they also disappear abruptly (Fig. 6).

Compared with ML the composition of the shorter AB core is dominated by Group 13/14 sandstones/siltstones/mudstone clasts (87%), with only 13 volcanic clasts present (out of 366). The high proportion of plutonic clasts (9%) relative to ML (3%) and CIB (1%) is due to the presence of seven highly weathered and three fresh granitic clasts (Fig. 7). The highly weathered clasts are likely to have been eroded from moraines and/or conglomerate deposits in the catchment (cf. Clapperton and Sugden, 1983). It is likely that weathered plutonic clasts in the core are derived from the moraine deposits along the lakeshore and the margins of ice-shelf. Possible shifts in rhyolite and tuffaceous clast distribution occur, but the paucity of clasts makes it difficult to judge whether these are significant and/or related to erosion from catchment deposits or transportation through the ice shelf. Interestingly, the lack of volcanic deposits on the floor of Ablation Valley (Elliott, 1975) appears to be reflected in the general lack of volcanic clasts in the AB core (Figs. 6 and 7).

Due to its isolation from ice-shelf transport processes, the clast diversity in the CIB core is low, with only four major clast types present (Fig. 6). There are no obvious shifts in clast-type and the clasts appear to have been deposited in well-defined pulses (e.g. in Unit D). The majority of the clasts are sedimentary (Fig. 7), with Group 13/14 sandstone/mudstone

clasts dominating (Fig. 6). The number of Group 23 light grey tuff clasts is significant (19%) and proportionately greater than the ML and AB cores. The lack of variety in the volcanic clasts present in the CIB core reflects the general lack of volcanic outcrops in the catchment strata. Tuffaceous outcrops of similar composition to Group 23 tuffs have been found in the CIB lake catchment (Fig. 2c). The only clast that might not come from a CIB catchment source is the single Group 22-I granodiorite clast at 176 cm (Fig. 6: circled point 4).

5. Clast geochemistry, isotopic composition and provenance

Geochemical and isotopic analyses were used to further subdivide the provenance of clasts in the ML core. The following section details geochemical and isotopic characteristics of the key lithological groups that constrain provenance and depositional processes in Moutonnée Lake. In summary, εNd_i values for primary igneous clasts range from –3.37 to 5.18 (Fig. 8). All the values, except for C142 (εNd_i=5.18), lie within the range of previous analyses from granites and grandiorites from the Palmer Land (Fig. 8) (Millar et al., 2001). Overall, the clasts scatter around an Rb-Sr reference isochron of c. 143 Ma, approximately in the middle of the 90-200 Ma age range of rocks from Alexander Island and Palmer Land (Table 3).

5.1 Primary Igneous Clasts

Primary igneous clasts have similar REE and isotope compositions to several well-studied rock types from NW Palmer Land. Combined REE and isotope data from, in particular, granitic, dioritic and Group 1/7 vitric tuff clasts are compatible with a well-defined source in NW Palmer Land. Although a source in central and western Alexander Island, active during the Late Cretaceous (c. 80-60 Ma), cannot be completely ruled out, a more extensive source in Palmer Land or post-subduction Alexander Island is unlikely because the primary igneous clasts analysed have Sr and Nd isotope compositions that are dissimilar to very young (<60 Ma) or very old (>228 Ma) Palmer Land plutonic rocks. It is not possible to distinguish igneous clasts derived from NW Palmer Land from those recycled through the Fossil Bluff Group using geochemical or isotopic data. Nevertheless, some clasts show signs of substantial weathering consistent with recycling through moraine deposits or the Fossil Bluff Group.

5.1.1 Plutonic clasts

The number of plutonic clasts in the ML core is relatively small. Nevertheless, clast compositions provide useful marker points for comparison with more numerous volcanic clasts and are the most directly compatible with existing Sr and Nd isotope reference data. Three plutonic clasts were analysed: two granites (C68B and C18D), which represent all granites found in the core, and one foliated diorite (A13), a rock-type that is known to outcrop in NW Palmer Land (Vaughan and

Millar, 1996; Vaughan et al., 1997). Extensive superficial iron-oxide staining on C18D suggests it has been recycled through Fossil Bluff Group strata or catchment moraines. Moreover, C18D can be distinguished geochemically from C68B (i.e. unweathered granites) by its characteristically large negative Europium anomaly (Table 3), indicative of plagioclase fractionation and/or weathering. The granitic and dioritic clasts analysed have contrasting Sr and Nd isotope compositions. HREE vs LREE data suggest the heavily weathered granite clast, C18D, is derived from a continental/intraplate magma source (Table 3), whilst its low negative εNd_i and high $^{87}Sr/^{86}Sr_i$ values are compatible with existing Late Triassic or Late Jurassic data (Fig. 8). Clast A13 (foliated diorite) has low positive εNd_i and very low $^{87}Sr/^{86}Sr_i$ values, firmly associated with data from NW Palmer Land Cretaceous plutonic outcrops (Fig. 8).

The granite clast found at 176 cm the CIB core is similar to sample KG.871.2 (hornblende granite sample) from Alexander Island. Furthermore, some of the weathered granitic clasts in the AB core have a similar composition/external appearance (i.e. well-rounded, iron-stained) to weathered granite pebbles from conglomeratic outcrops in Ablation Valley in the BAS archives. With mean roundness of 2.4±0.4 and 43% equant clasts they are distinct from the more angular weathered granite clasts (1.5±0.6; 0%; Table 2) found in the ML core, and perhaps indicative of a different mode of transport, for example, multiple-phase reworking from local moraines rather than first phase input from local outcrops (Elliott, 1975; Bishop and Walton, 1981; Clapperton and Sugden, 1983; Smith et al., 2006).

5.1.2 Volcanic clasts

The original source and final depositional provenance and evaluation of ice shelf retreat/reformation processes is based primarily on key rhyolitic and tuff clast types. Seventeen volcanic clasts, representing 12 different lithological types, were analysed. Group 2, 3 rhyolites and Group 1/7 olive/dark vitric tuff/lava clasts are the most significant clast types. In ML, they occur throughout marine zones 2-4 in roughly equal proportions to sedimentary clasts and dominate the epishelf Zone 5 sediments, yet they appear only sporadically in the AB core and are completely absent from the CIB core.

Group 2 and 3 Rhyolites: Two clasts, one from each group, were analysed. Both are medium-K subalkaline tholeiites of the calc-alkaline series. Major/trace and REE compositions and Eu/Eu* values of Group 2 and 3 rhyolites are similar (Table 3). Sr and Nd isotope data shows they have a different eruption age and/or source (Fig. 8; Table 3). Group 2 rhyolites (e.g. C71) are characterised by low negative εNd_i and high $^{87}Sr/^{86}Sr_i$ values typically associated with Late Triassic or Mid-Late Jurassic igneous rocks from Palmer Land (Fig. 8) (Millar et al., 2001). In contrast, Group 3 rhyolites (e.g. C83) have low positive εNd_i/low $^{87}Sr/^{86}Sr_i$ values more typically associated with Late Cretaceous igneous complexes of NW Palmer Land (Fig. 8). No Group 3 rhyolite specimens from the Ablation Point area were found in the BAS

archives, suggesting a restricted, but as yet undiscovered, outcrop in the Moutonnée Valley area or transportation through George VI Ice Shelf.

Several factors indicate that Group 3 rhyolites are most likely eroded from the ML catchment: (i) the simultaneous input of Group 3 rhyolites and Group 1/7 clasts in Zone 5 of the ML core, (ii) their lack of striations, less well-rounded shape, the small proportion of Group 3 weathered rhyolites (10% vs 18%) relative to Group 2 rhyolites (Table 2), (iii) a possible shift from Group 2 to Group 3 rhyolites in the AB core (iv) an absence of Group 2 rhyolites in all but the basal 5 cm of the AB core. Moreover, if both types of rhyolite were eroded directly from Alexander Island outcrops or moraines it is likely that both types would be represented in the epishelf lake sediments of Zone 5 of the ML core.

Group 1/7 vitric tuffs: Group 1 tuff clasts are dark olive-green volcanic tuffs with 1-3 mm black ash/scoraceous deposits. In thin section, much of the groundmass is fine-grained/unidentifiable or composed of plagioclase and/or glassy fragments. The presence of secondary flow patterns and a well-preserved hyaloclastite texture, that has not been recrystallised, suggests a subglacial eruption or thermal shocking in contact with water, both compatible with a magmatic arc REE source classification.

Sr and Nd isotope analysis shows the original source of Group 1/7 clasts has a strong affinity with Palmer Land Cretaceous plutonic data (Fig. 8). However, their final source, prior to deposition into the lake, during the Holocene was probably local, i.e., Alexander Island. Group 7 tuff clasts are distinguished from Group 1 clasts by higher proportions of plagioclase phenocrysts and their associated positive Europium anomalies (Table 3). Combined, group 1/7 clasts form an evolutionary trend within the transitional alkaline series and exhibit negative relationship between Eu/Eu* and silica content, reflecting increasing plagioclase fractionation from the melt (Fig. 8). They are clearly distinct from alkaline (C124: Grp. 19) and subalkaline (tholeiitic) (C270A: Grp. 28) dark green lava clasts, but have εNd and $^{87}Sr/^{86}Sr_i$ values that are similar those of the foliated diorite clast A13, suggesting a well-defined NW Palmer Land source. Agglomerative hierarchical cluster analysis of all igneous clast εNd_i, $^{87}Sr/^{86}Sr_i$ and Rb/Sr data produces nine distinct cluster groups. Overall, no relationship exists between the different clast types in each cluster group, but it is interesting to note data from Group 1/7 clasts, C124, a trachyandesitic dark green lava, and A13 are closely related statistically.

The evolutionary relationships between Group 1/7 clasts could reflect a single eruption event, or a similar eruption source. The low to medium positive εNd_i and low $^{87}Sr/^{86}Sr_i$ values indicate that olive/dark green tuffs and lava clasts are primarily derived from mantle sources with relatively little assimilation of older crust compared to other igneous clasts

(Table 3). Their isotopic composition is compatible with Late Jurassic-Early Cretaceous plutonic rocks from NW Palmer Land (Fig. 8) (Wareham et al., 1997; Millar et al., 2001) and outcrops with similar petrology in northern Palmer Land (Smith, 1987).

Rock specimens of Group 1/7 vitric tuffs and dark green lavas from Moutonnée and Ablation Valley are well represented in the BAS archive collection. For example, the green vitric lava clast C124 is similar in hand specimen to sample KG802.1, a dark green fine-grained lava with dark chlorite filled amygdales, from the Himalia Ridge (Fig. 2b). Unlike AB and CIB, unidirectional glacially striated volcanic rocks (e.g. KG.853) and till deposits outcrop extensively on the gravel-covered valley floor around Moutonnée Lake and volcanic deposits are common in adjacent screes and moraines (Elliott, 1974; Clapperton and Sugden, 1982; Clapperton and Sugden, 1983) .

The presence of tuff deposits similar to Groups 1/7 in agglomerate sample KG.804.1 suggests Group 1/7 tuffs were syndepositionally emplaced then reworked into the sedimentary deposits of Alexander Island. Moreover, substantial iron oxide weathering on specimens equivalent to Group 1/7 clasts (e.g. KG.877.1, KG.853.2 and KG.801.1) suggests derivation from conglomerate/agglomerate beds of the Fossil Bluff Group and/or moraine deposits within or at the entrance to Moutonnée Valley (cf. Clapperton and Sugden, 1983).

5.2 Secondary clasts

5.2.1 Secondary volcanic clasts

Most significant are Group 23 grey/white volcanic tuffs/tuffaceous sandstones, which are present in all three cores. Greater than 70% of clasts of this type are found in the CIB core. Their presence throughout the core (and in the ML and AB cores) would suggest derivation from exposed strata from within the FBG in the CIB catchment rather than transportation from distal sources. Significantly, the arkosic sandstones and pebbly arkosic sandstones of the FBG contain heavily reworked/well rounded igneous clasts of pebble grade, similar to the granitic clasts found in the ML and AB cores. In the ML core, >80% of Group 23 clasts were found in the IRD Zone 3, but were notably absent from Zone 5 sediments. This likely reflects a significant change in the erosion source of (advancing?) catchment glaciers, sourcing of different strata within the Fossil Bluff Group and/or the relatively limited number of grey/white volcanic tuff outcrops in Moutonnée and Ablation Valley compared to the Citadel Bastion catchment.

5.2.2 Sedimentary clasts

It is likely that sedimentary clasts are exclusively derived from the Fossil Bluff Group (FBG) strata on Alexander Island. In this respect, their provenance relationships are not diagnostic of changing depositional processes. Sedimentary clasts are predominantly greywackes and shales. Exceptions are A8 and C11, which are litharenites and C187 which is an Fe-Sand (cf. Herron, 1988). REE data from For Group 14 mudstones show that this lithology is characterised by a significant positive Europium anomaly (Table 3). The distribution of sandstones analysed in this study is similar to those from the Pluto and Neptune Glacier Formations (cf. Browne, 1996). The geochemistry of the <63 μm silt and clay fraction in the ML core is most similar to major element compositions of C522, C512 and C11, i.e. Group 14 black mudstones and Group 16/26 white/grey sandstones. These are from layered outcrops that constitute most of the Fossil Bluff Group.

6. Discussion

6.1 Eruption sources, age and tectonic setting

Most rocks eroding from Palmer Land are c. 100-140 Ma. Two clasts, C71 (Group 2, Type I rhyolite) and C18d (Group 22-III granite) form trendlines that are significantly older than the average clast age of c.140 Ma. An estimated age of c. 180 Ma links them with Late Triassic-Upper Jurassic formations in Palmer Land.

6.1.1 Primary clasts

The majority of the igneous clasts plot within the magmatic arc domain for AP rocks on HREE vs LREE (Th/Yb vs Ta/Yb and Th/Ta vs La/Ta) ratio plots McCarron and Smellie (1998) used to define magmatic sources of Antarctic Peninsula rocks. The two exceptions are C18D (Group 22 granite) and C13A (Group 1 olive green crystal tuff). Sr and Nd isotope data indicates these clasts could be derived from intraplate magmas or the Jurassic-mid Cretaceous Lemay Group of Alexander Island (Doubleday, 1994).

Unaltered, crystal-rich volcanic tuffs and fine-grained rhyolites (e.g. Groups 1/7, 2, 3) reflect the age and location of source volcanism. Late Jurassic-Early Cretaceous (141-127 Ma) granitoid rocks of the western Palmer Land Central Domain are derived from the mantle, or by melting of underplate, and have low initial Sr ratios and high εNd_i values, while older rocks, which have assimilated continental crust, have higher initial Sr ratios and lower/negative εNd_i values (Millar et al., 2001). Rb-Sr and Nd isotope data indicate that these clast types probably originated from volcanic rocks from in Palmer Land, most likely during a period of widespread and intensive Early Cretaceous arc-related volcanism at around 140 Ma. (Millar et al., 2001).

6.1.2 Secondary and sedimentary clasts

Secondary and sedimentary clasts (e.g. lithic-rich tuffs and tuffaceous sandstone clasts) are not diagnostic indicators of eruption age or source because they contain a large component of reworked sedimentary material. The Sr and Nd isotope composition more than likely reflects the c. 140 Ma average age of rocks from NW Palmer Land and Alexander Island. All non igneous clasts and sediments sand-silt fraction sediments from the ML core plot in either arc related or active continental margin fields (Bhatia, 1983; Roser and Korsch, 1986).

6.2 Depositional model & modes

Based on detailed on-site investigation, Smith et al. (2006) have proposed a combined biological, geochemical and lithological conceptual model for detecting periods of ice shelf loss from the analysis of epishelf lake sediments (Fig. 3). In this model, periods of ice-shelf presence are defined by a restricted range of clast lithologies and clast provenance (mainly catchment-derived rocks plus some input from specific locations upstream of the main ice shelf flow lines). In contrast, periods of ice shelf absence would result in a wider range of clast lithologies sourced from a wider region incorporating both rocks from Alexander Island and rock from further a field transported to the site as ice rafted debris.

Lithological and clast isotopic provenance analyses allow us to develop this model further. Six modes of clast deposition in Moutonnée Lake are summarised in Table 4. These reflect: (i) clast source areas; (ii) erosion and depositional processes; (iii) the relative influence/depositional potential of catchment glaciers vs ice shelf transport; and (iv) changes in the strength and/or direction of ice shelf flow pathways into the lakes.

Some caution has to be exercised, however, when assigning specific provenance locations and modes of deposition. Absolute determinations of source remain elusive for many clast types for the following reasons:

(i) The principal difficulty in identifying provenance of the sedimentary clasts is the bimodal provenance signal from the accretionary complex and volcanic arc that was active in Palmer Land at the time. The petrography of sediments in the Alexander Island mega basin sequence reflect coeval arc volcanism, and erosion of older Palmer Land volcanic outcrops. Volcanic deposits in the Fossil Bluff Group or along Moutonnée Valley were derived from the rocks of the Central Domain, but could be related to ash/tuffs that were deposited synformationally (Horne, 1968). In both cases, the isotopic signature will be the same as near source igneous outcrops in Palmer Land. Similarly, the lower Cretaceous sandstones and conglomerates of the Alexander Island sediments were thought to have been derived from an elevated source area composed of granodioritic, parametamorphic and volcanic rocks (Butterworth, 1991; Browne, 1996).

(ii) Relative to Palmer Land, there are few volcanic outcrops in the lake catchment strata. Tuff and ash deposits in the top of the Himalia Ridge and Spartan Glacier Formations are most likely products of Late Cretaceous/Early Tertiary eruptions from Alexander Island and/or coeval volcanism in Palmer Land.

(iii) Reworked AP erratics (primarily granites) and granitic rocks associated with the Himalia Formation of Alexander Island have been found in conglomerate and moraine sequences of the Ablation Point massif and along the Moutonnée Lake shoreline (Clapperton and Sugden, 1982; Clapperton and Sugden, 1983; Smith et al., in press). Reworked clasts were distinguished from freshly eroded/exotic clasts to some extent by their highly weathered, rounded and/or iron stained appearance. This is not entirely diagnostic and it is possible that clasts could be from unweathered or unexposed parts of such deposits.

(iv) Major/trace and REE data from the Fossil Bluff Group is limited. Further isotopic work that might tighten clast source areas is in progress and it may be possible to pinpoint source outcrops more accurately in future (e.g. Flowerdew et al., 2003).

(iv) Palmer Land analyses were undertaken on granites, granodiorites and tonalities. GVIIS analyses were undertaken on available clast types. These were dominated by tuffs and rhyolites and sedimentary clasts that may not be directly related to the Palmer Land crustal evolution. This study is different to most geological investigations because it was not possible to select, *a priori*, the most suitable rock types for analyses. Certain volcanic clasts (e.g. tuffs) and bulk compositions are not necessarily diagnostic of a particular source.

Nevertheless, there is a clear difference in lithology and geochemistry of the clasts deposited in the marine ML Zones 2-4 compared with clasts from the other zones in the ML core and from the reference cores (CIB, AB). Specifically the melange of clast types of predominantly medium (10-50 g) to large (>50 g) mass in Zone 3 follows the first incursion of marine water (Zone 2) and suggests that the ice shelf dam and lake ice had disappeared allowing icebergs from George VI Sound to drift into the newly formed marine embayment and deposit ice rafted debris. The assemblage in Zone 4 is initially dominated (to c. 270 cm depth; c. 8500 ka BP) by local Group 14 mudstones/siltstones of the FBG, but the fine sediments deposited in the latter half of this zone suggest ice-rafting was not the dominant sedimentary process c. 8500-7500 yr. BP. The switch to an assemblage dominated by Group 1/7 olive green vitric tuff clasts in Zone 5 suggests IRD/marine deposition processes ceased at this time and instead were replaced by local glaciers from Moutonnée Valley, calving directly into the newly formed marine embayment, and depositing locally-sourced volcanic material.

6.3 Relationship to wider events

Clapperton and Sugden (1982) constructed a preliminary Holocene glacial history for George VI Sound from geomorphological relationships between till deposits, moraines, radiocarbon and amino acid racemization ages from barnacles in moraines deposits. Their radiocarbon ages suggested open water conditions existed in George VI Sound at

least until c. 6500 ^{14}C yr B.P. (c. 6000 cal yr BP – 2σ median probability, using same input factors as Bentley et al., 2005) with four phases of valley glacier advance including an advance phase prior to c. 6000 yr. BP.

Without accurate age constraints in the upper half of the ML core it is not possible to categorically assign gaps in the down core distribution of olive/dark green rhyolitic and tuffaceous clasts between 236-44 cm to climatically induced changes in glacial activity. Nevertheless, six phases of increased Group 1/7 clast density exist. This suggests up to five phases of increased glacial activity, some of which could be contemporaneous with the four phases of valley glacier advance proposed by Clapperton and Sugden (1982). Phases of increased Group 1/7 clast density are indicative, perhaps, of pulsed deposition from stagnating lake ice, calving-related deposition in the near-shelf area of the lake and/or fluctuations at its margin related to retreat of catchment glaciers, perhaps during periods of precipitation decline.

Shifts in clast data associated with the transition from marine embayment to epishelf lake conditions support our previous conclusion (Bentley et al., 2005) that GVIIS was absent from the Ablation Point area between 9595 and 7945 cal. yr. BP. This retreat occurred immediately after a period of maximum Holocene warmth documented in the EPICA Dome C ice core record (Masson-Delmotte et al., 2004) and at the same time as an influx of warmer Circumpolar Deep Water onto the continental shelf (Domack et al., 2001; Bentley at al., 2005). Not long after the initial ice-shelf break up, ice-rafted debris was deposited into ML. Subsequent reformation of the ice-shelf occurred at the same time period as a the Holocene climatic minimum in the EPICA Dome C ice core (Masson-Delmotte et al., 2004). There is no clear evidence of substantial phases of retreat or a return to marine conditions during the well-documented, and prolonged, 'mid-Holocene warm period' (Hodgson et al., 2004), when conditions were warm enough to cause significant retreat of ice shelves across the northern AP (Domack et al., 1999; Domack et al., 2001; Pudsey and Evans, 2001; Taylor et al., 2001; Hodgson et al., 2004).

7. Conclusions

- Clasts >8 mm in cores from three lakes on eastern Alexander Island can provide a proxy measure of changes in the configuration of GVIIS. The Moutonnée Lake core has significant changes in clast type and density that are coupled to retreat phases of GVIIS and, most likely, readvance phases of local catchment glaciers in Moutonnée Valley.

- The early Holocene retreat of GVIIS in the Ablation Point area (Bentley et al., 2005) is marked by a distinct depositional shift from a more 'ordered' assemblage and low number of clast types when the ice shelf is present to a more chaotic distribution of clasts and more numerous clast types during the period when the ice-shelf was absent.

During periods of ice-shelf loss, the lithological assemblage is dominated a range of exotic clasts. Iceberg rafting of material is likely to be the dominant sedimentary process during periods of ice-shelf loss. Subglacial flow through the ice-shelf is relatively minor compared to the input of material from local catchment glaciers and iceberg rafting.

- Further isotopic and age analyses of volcanic outcrops on Alexander Island and NW Palmer Land are necessary to determine provenance more precisely. This is a substantial undertaking, beyond the scope of this paper. Nevertheless, data presented in this paper have identified six modes of clast transport highlighting the complex provenance and depositional processes in Moutonnée Lake and the GVIIS-epishelf lake sedimentary system along the eastern coast of Alexander Island.

Acknowledgements: This study was funded by the BAS core program 'Signals in Antarctica of past Global ChangeS' (SAGES)-10K, the NERC Antarctic Funding Initiative project (AFI2/69 and CGS00/06) with additional support from the NERC Radiocarbon Laboratory, East Kilbride, the NERC Isotope Geosciences Laboratory, Keyworth. Thanks to: Alex Tate (BAS Geological Database); Mike Tabecki (BAS rock archive); Charlotte Bryant, Alan Vaughan, Phil Leat (discussions/assistance). Thanks also to Pete Milner, Adam Hunt and BAS Field Operations Staff for assistance in the field, MAGIC (BAS: Peter Fretwell and Andreas Cziferszky) for additional field data from Citadel Bastion, maps and photos, and Dodie James (Edinburgh) for assistance with XRF analysis. This paper benefited greatly from constructive reviews by Bob Gilbert and Eugene Domack, for which we are grateful.

References

Anderson, J.B., Shipp, S.S., Lowe, A.L., Wellner, J.S. and Mosola, A.B., 2002. The Antarctic Ice Sheet during the Last Glacial Maximum and its subsequent retreat history: a review. Quaternary Science Reviews, 21(1-3): 49-70.

Andrews, J.T. and Principato, S.M., 2002. Grain-size characteristics and provenance of ice-proximal marine sediments. In: J.A. Dowdeswell and C. Ó Cofaigh (Editors), Glacier-influenced Sedimentation on High-Latitude Continental Margins. Geological Society, Special Publications, London, pp. 305-324.

Bell, A.C. and King, E.C., 1998. New seismic data support Cenozoic rifting in George VI Sound, Antarctic Peninsula. Geophysical Journal International, 134(3): 889-902.

Bentley, M.J., Hodgson, D.A., Sugden, D.E., Roberts, S.J., Smith, J.A., Leng, M.J. and Bryant, C., 2005. Early Holocene retreat of the George VI Ice Shelf, Antarctic Peninsula. Geology, 33(3): 173-176.

Berkman, P. A. and Forman, S. L., 1996. Pre-bomb radiocarbon and the reservoir correction for calcareous marine species in the Southern Ocean. Geophysical Research Letters 23(4): 363-366.

Bhatia, M.R., 1983. Plate tectonics and geochemical composition of sandstones. Journal of Geology, 91: 611-627.

Bishop, J.F. and Walton, J.L.W., 1981. Bottom melting under George VI Ice Shelf, Antarctica. Journal of Glaciology, 27: 429-447.

Brachfeld, S., Domack, E., Kissel, C., Laj, C., Leventer, A., Ishman, S., Gilbert, R., Camerlenghi, A. and Eglinton, L.B., 2003. Holocene history of the Larsen-A Ice Shelf constrained by geomagnetic paleointensity dating. Geology, 31(9): 749-752.

Browne, J., 1996. Sandstone provenance and diagenesis of arc-related basins: James Ross Island and Alexander Island, Antarctica. PhD Thesis, University of Exeter, Exeter, 464 pp.

Butterworth, P.J., 1991. The role of eustasy in the development of a regional shallowing event in a tectonically active basin: Fossil Bluff Group (Jurassic-Cretaceous), Alexander Island, Antarctica. In: D.I.M. Macdonald (Editor), Sedimentation, Tectonics and Eustasy. Special Publication of the International association of Sedimentologists. Blackwell Scientific Publications, Oxford, pp. 307-329.

Clapperton, C.M. and Sugden, D.E., 1982. Late Quaternary glacial history of George VI Sound area, West Antarctica. Quaternary Research, 18: 243-267.

Clapperton, C.M. and Sugden, D.E., 1983. Geomorphology of the Ablation Point massif, Alexander Island, Antarctica. Boreas, 12: 125-135.

Cook, A.J., Fox, A.J., Vaughan, D.G. and Ferrigno, J.G., 2005. Retreating glacier fronts on the Antarctic Peninsula over the past half-century. Science, 308: 541-544.

De Angelis, H. and Skvarca, P., 2003. Glacier surge after ice shelf collapse. Science, 299: 1560-1562.

Depaolo, D.J., Linn, A.M. and Schubert, G., 1991. The Continental Crustal Age Distribution - Methods of Determining Mantle Separation Ages from Sm-Nd Isotopic Data and Application to the Southwestern United-States. Journal of Geophysical Research-Solid Earth and Planets, 96(B2): 2071-2088.

Doake, C.S.M., Corr, H.F.J., Rott, H., Skvarca, P. and Young, N.W., 1998. Breakup and conditions for stability of the northern Larsen Ice Shelf, Antarctica. Nature, 391: 778-780.

Domack, E., Duran, D., Leventer, A., Ishman, S., Doane, S., McCallum, S., Amblas, D., Ring, J., Gilbert, R. and Prentice, M., 2005. Stability of the Larsen B ice shelf on the Antarctic Peninsula during the Holocene epoch. Nature 436: 681-685.

Domack, E., Leventer, A., Dunbar, R., Taylor, F., Brachfeld, S. and Sjunneskog, C., 2001. Chronology of the Palmer Deep site, Antarctic Peninsula: a Holocene palaeoenvironmental reference for the circum-Antarctic. The Holocene, 11(1): 1-9.

Domack, E.W., Jacobson, E.A., Shipp, S. and Anderson, J.B., 1999. Late Pleistocene-Holocene retreat of the West Antarctic Ice- Sheet system in the Ross Sea: Part 2 - Sedimentologic and stratigraphic signature. Geological Society of America Bulletin, 111(10): 1517-1536.

Doran, P.T., Berger, G.W., Lyons, W.B., Wharton Jr., R.A., Davisson, M.L., Southon, J. and Dibb, J.E., 1999. Dating Quaternary lacustrine sediments in the McMurdo Dry Valleys, Antarctica. Palaeogeography, Palaeoclimatology, Palaeoecology, 147(3-4): 223-239.

Doubleday, P.A., 1994. Structural and tectonic evolution of parts of the Mesozoic forearc of Alexander Island. PhD Thesis, University of Leeds, 292 pp.

Doubleday, P.A., Macdonald, D.I.M. and Nell, P.A.R., 1993. Sedimentology and Structure of the Trench-Slope to Fore-Arc Basin Transition in the Mesozoic of Alexander Island, Antarctica. Geological Magazine, 130(6): 737-754.

Elliott, M.H., 1974. Stratigraphy and sedimentary petrology of the Ablation Point area, Alexander Island. British Antarctic Survey Bulletin, 39: 87-113.

Elliott, M.H., 1975. The stratigraphy and sedimentary petrology of the Ablation Point area, Alexander Island. MSc. Dissertation, University of Birmingham, 93 pp.

Evans, J. and Pudsey, C.J., 2002. Sedimentation associated with Antarctic Peninsula ice shelves: implications for palaeoenvironmental reconstructions of glacimarine sediments. Journal of the Geological Society, London, 159: 233-237.

Flowerdew, M.J., Millar, I.L. and Vaughan, A.P.M., 2003. Does the Antarctic Peninsula comprise exotic terranes? Hf isotope analysis from detrital and magmatic zircons, Antarctic Funding Initiative (AFI) Conference (http://www.antarctica.ac.uk/afi/abstracts.htm), Cambridge.

Gilbert, R. and Domack, E.W., 2003. Sedimentary record of disintegrating ice shelves in a warming climate, Antarctic Peninsula. Geochemistry Geophysics Geosystems, 4: art. no.-1038.

Govindaraju, K., 1994. 1994 Compilation of Working Values and Sample Description for 383 Geostandards. Geostandards Newsletter, 18(Special Issue): 1.

Hendy, C.H., 2000. The role of polar lake ice as a filter for glacial lacustrine sediments. Geografiska Annaler, 82(2-3): 271-278.

Hendy, C.H. and Hall, B.L., 2006. The radiocarbon reservoir effect in proglacial lakes: Examples from Antarctica. Earth and Planetary Science Letters, 241(3-4): 413-421.

Herron, M.M., 1988. Geochemical Classification of Terrigenous Sands and Shales from Core or Log Data. Journal of Sedimentary Petrology, 58(5): 820-829.

Heywood, R.B., 1977. A limnological survey of the Ablation Point area, Alexander Island, Antarctica. Philosophical Transactions of the Royal Society of London, B279: 39-54.

Hodgson, D.A., Doran, P.T., Roberts, D. and McMinn, A., 2004. Paleolimnological studies from the Antarctic and sub Antarctic islands. In: R. Pienitz, M.S.V. Douglas and J.P. Smol (Editors), Developments in Palaeoenvironmental Research. Volume 8. Long-term Environmental Change in Arctic and Antarctic Lakes. Kluwer, Dordrecht, pp. 550.

Horne, R.R., 1968. Petrology and provenance of the Cretaceous sediments of south-eastern Alexander Island. British Antarctic Survey Bulletin, 17: 73-82.

Howe, J., 2003. Mid Cretaceous fossil forests of Alexander Island, Antarctica. PhD Thesis, University of Leeds, 200 pp.

Jones, V.J., Hodgson, D.A. and Chepstow-Lusty, A., 2000. Palaeolimnological evidence for marked Holocene environmental changes on Signy Island, Antarctica. The Holocene, 10(1): 43-60.

King, J.C., Turner, J., Marshall, G.J., Connolly, W.M. and Lachlan-Cope, T.A., 2004. Antarctic Peninsula Climate Variability and its Causes as Revealed by Analysis of Instrumental Records. In: E. Domack et al. (Editors), Antarctic Peninsula Climate Variability: Historical and Paleoenvironmental Perspectives. Antarctic Research Series. American Geophysical Union, pp. 272.

Kuhn, G., Melles, M., Ehrmann, W.U., Hambrey, M.J. and Schmiedl, G., 1993. Character of clasts in glaciomarine sediments as an indicator of transport and depositional processes, Weddell and Lazarev Seas, Antarctica. Journal of Sedimentary Petrology, 63(3): 477-487.

Leat, P.T., Scarrow, J.H. and Millar, I.L., 1995. On the Antarctic Peninsula Batholith. Geological Magazine, 132(4): 399-412.

Lewis, T., Gilbert, R. and Lamoureux, S.F., 2002. Spatial and temporal changes in sedimentary processes in proglacial Bear Lake, Devon Island, Nunavut, Canada. Arctic, Antarctic, and Alpine Research, 34: 119-129.

Ludwig, K.R., 2003. Isoplot 3.00: A geochronological toolkit for Microsoft Excel, Special Publication No. 4. Berkeley Geochronology Center, 71 pp.

Macdonald, D.I.M., Moncrieff, A.C.M. and Butterworth, P.J., 1993. Giant Slide Deposits from a Mesozoic Fore-Arc Basin, Alexander Island, Antarctica. Geology, 21(11): 1047-1050.

Masson, V., Vimeux, F., Jouzel, J., Morgan, V., Delmotte, M., Ciais, P., Hammer, C., Johnsen, S., Lipenkov, V.Y., Mosley-Thompson, E., Petit, J.R., Steig, E.J., Stievenard, M. and Vaikmae, R., 2000. Holocene climate variability in Antarctica based on 11 ice-core isotopic records. Quaternary Research, 54(3): 348-358.

Masson-Delmotte, V., Stenni, B. and Jouzel, J., 2004. Common millennial-scale variability of Antarctic and Southern Ocean temperatures during the past 5000 years reconstructed from the EPICA Dome C ice core. Holocene, 14(2): 145-151.

McCarron, J.J. and Millar, I.L., 1997. The age and stratigraphy of fore-arc magmatism on Alexander Island, Antarctica. Geological Magazine, 134(4): 507-522.

McCarron, J.J. and Smellie, J.L., 1998. Tectonic implications of fore-arc magmatism and generation of high-magnesian andesites: Alexander Island, Antarctica. Journal of the Geological Society, 155: 269-280.

Millar, I.L., Willan, R.C.R., Wareham, C.D. and Boyce, A.J., 2001. The role of crustal and mantle sources in the genesis of granitoids of the Antarctic Peninsula and adjacent crustal blocks. Journal of the Geological Society, 158: 855-867.

Miller, S. and Macdonald, D.I.M., 2004. Metamorphic and thermal history of a fore-arc basin: the Fossil Bluff Group, Alexander Island, Antarctica. Journal of Petrology, 45(7): 1453-1465.

Moncrieff, A.C.M. and Kelly, S.R.A., 1993. Lithostratigraphy of the Uppermost Fossil Bluff Group (Early Cretaceous) of Alexander Island, Antarctica - History of an Albian Regression. Cretaceous Research, 14(1): 1-15.

Norrish, K. and Hutton, J.T., 1969. An accurate X-ray spectrographic method for the analysis of a wide range of geological samples. Geochemica et Cosmochimica Acta, 33: 431-453.

O Cofaigh, C.O., Dowdeswell, J.A. and Pudsey, C.J., 2001. Late Quaternary iceberg rafting along the Antarctic Peninsula continental rise and in the Weddell and Scotia Seas. Quaternary Research, 56(3): 308-321.

Olive, V., Ellam, R.M. and Wilson, L., 2001. A protocol for the determination of the rare Earth elements at picomole level in rocks by ICP-MS: Results on geological reference materials USGSPCC-1 and DTS-1. Geostandards Newsletter, 25: 219-288.

Pankhurst, R.J., 1982. Rb-Sr Geochronology of Graham Land, Antarctica. Journal of the Geological Society, 139(NOV): 701-711.

Pankhurst, R.J., 1990. The Paleozoic and Andean magmatic arcs of West Antarctica and southern America. Geological Society of America, Special Paper, 241: 1-7.

Pankhurst, R.J., Millar, I.L., Grunow, A.M. and Storey, B.C., 1993. The Pre-Cenozoic Magmatic History of the Thurston Island Crustal Block, West Antarctica. Journal of Geophysical Research-Solid Earth, 98(B7): 11835-11849.

Pearson, M.R. and Rose, I.H., 1983. The dynamics of George VI Ice Shelf. British Antarctic Survey Bulletin, 52: 205-220.

Pettijohn, F.J., Potter, P.E. and Siever, R., 1987. Sand and Sandstone. Springer-Verlag, New York, 553 pp.

Potter, J.E. and Paren, J.G., 1985. Interaction between ice shelf and ocean in George VI Sound, Antarctica. In: S.S. Jacobs (Editor), Oceanology of the Antarctic continental shelf. Antarctic Research Series, pp. 35-58.

Pudsey, C.J., 2000. Sedimentation on the continental rise west of the Antarctic Peninsula over the last three glacial cycles. Marine Geology, 167: 313-338.

Pudsey, C.J., Barker, P.F. and Larter, R.D., 1994. Ice-Sheet Retreat from the Antarctic Peninsula Shelf. Continental Shelf Research, 14(15): 1647-1675.

Pudsey, C.J. and Evans, J., 2001. First survey of Antarctic sub-ice shelf sediments reveals mid- Holocene ice shelf retreat. Geology, 29(9): 787-790.

Roser, B.P. and Korsch, R.J., 1986. Determination of Tectonic Setting of Sandstone-Mudstone Suites Using Sio2 Content and K2o Na2o Ratio. Journal of Geology, 94(5): 635-650.

Saunders, A.D., Tarney, J. and Weaver, S.D., 1980. Transverse Geochemical Variations across the Antarctic Peninsula - Implications for the Genesis of Calc-Alkaline Magmas. Earth and Planetary Science Letters, 46(3): 344-360.

Scambos, T.A., Bohandler, J., Shuman, C.A. and Skvarca, P., 2004. Glacier acceleration and thinning after ice shelf collapse in the Larsen B Embayment, Antarctica. Geophysical Research Letters, 31: L18402, doi:10.1029/2004GL0260670.

Scambos, T.A., Hulbe, C., Fahnestock, M. and Bohandler, J., 2000. The link between climate warming and break-up of ice shelves in the Antarctic Peninsula. Journal of Glaciology, 46: 516-530.

Shepherd, A., Wingham, D., Payne, T. and Skvarca, P., 2003. Larsen ice shelf has progressively thinned. Science, 302: 856-859.

Smith, C.G., 1987. The geology of parts of the west coast of Palmer Land. British Antarctic Survey Scientific Reports, 112: 101.

Smith, J.A., Bentley, M.J., Hodgson, D.A., Roberts, S.J., Verleyen, E., Leng, M.J., Lloyd, J.M., Barrett, M.J., Bryant, C. and Sugden, D.E., in press. Oceanic and atmospheric forcing of early Holocene ice shelf retreat, George VI Ice Shelf, Antarctic Peninsula. Quaternary Science Reviews.

Smith, J.A., Hodgson, D.A., Bentley, M.J., Verleyen, E., Leng, M.J. and Roberts, S.J., 2006. Limnology of Two Antarctic Epishelf Lakes and their Potential to Record Periods of Ice Shelf Loss. Journal of Paleolimnology, 35(2): 373-394.

Storey, B.C., Brown, R.W., Carter, A., Doubleday, P.A., Hurford, A.J., Macdonald, D.I.M. and Nell, P.A.R., 1996. Fission-track evidence for the thermotectonic evolution of a Mesozoic-Cenozoic fore-arc, Antarctica. Journal of the Geological Society, 153: 65-82.

Stuiver, M. and Reimer, P.J., 1993. Extended 14C database and revised CALIB radiocarbon calibration program. Radiocarbon, 35: 215-230.

Stuvier, M., et al., 1998. INTCAL98 radiocarbon calibration 24,000-0 cal BP. Radiocarbon, 40, 1041-1083.

Suarez, M., 1976. Plate-Tectonic Model for Southern Antarctic Peninsula and Its Relation to Southern Andes. Geology, 4(4): 211-214.

Taylor, F., Whitehead, J. and Domack, E., 2001. Holocene paleoclimate change in the Antarctic Peninsula: evidence from the diatom, sedimentary and geochemical record. Marine Micropaleontology, 41(1-2): 25-43.

Tucker, M.E., 1981. Sedimentary petrology: An introduction to the origin of sedimentary rocks. Blackwell, Oxford, 260 pp.

Vaughan, A.P.M. and Millar, I.L., 1996. Early Cretaceous magmatism during extensional deformation within the Antarctic Peninsula magmatic arc. Journal of South American Earth Sciences, 9(1-2): 121-129.

Vaughan, A.P.M. and Storey, B.C., 2000. The eastern Palmer Land shear zone: a new terrane accretion model for the Mesozoic development of the Antarctic Peninsula. Journal of the Geological Society, 157: 1243-1256.

Vaughan, A.P.M., Wareham, C.D. and Millar, I.L., 1997. Granitoid pluton formation by spreading of continental crust: the Wiley Glacier complex, northwest Palmer Land, Antarctica. Tectonophysics, 283(1-4): 35-60.

Vaughan, D.G. and Doake, C.S.M., 1996. Recent atmospheric warming and retreat of ice shelves on the Antarctic Peninsula. Nature, 379: 328-331.

Vaughan, D.G., Marshall, G.J., Connolley, W.M., Parkinson, C., Mulvaney, R., Hodgson, D.A., King, J.C., Pudsey, C.J. and Turner, J., 2003. Recent rapid regional climate warming on the Antarctic Peninsula. Climatic Change, 60(3): 243-274.

Vermeesch, P., 2004. How many grains are needed for a provenance study? Earth and Planetary Science Letters, 224(3-4): 441-451.

Wareham, C.D., Millar, I.L. and Vaughan, A.P.M., 1997. The generation of sodic granite magmas, western Palmer Land, Antarctic Peninsula. Contributions to Mineralogy and Petrology, 128(1): 81-96.

Figures and Tables

Figures

Fig. 1 Location map showing the position of Moutonnée Lake, Ablation Lake and Citadel Bastion Lake on Alexander Island, Antarctic Peninsula. The position of some former ice shelves are marked together with dates of their most recent collapse events.

Fig. 2 Geomorphological maps and aerial photographs of: **(a, b)** Ablation Lake and Moutonnée Lake showing where the ice of George VI Ice Shelf forms a dam across the mouths of Moutonnée and Ablation valleys and illustrating the relative lack of lake-proximal glacial activity in Moutonnée Valley compared to Ablation Valley and **(c)** Citadel Bastion lake showing the coring site and its separation from George VI Ice Shelf. KG sample numbers refers to the location of rocks in the BAS geological database. Locations A-H refer to sites discussed in the text and relate to original outcrops mapped by Elliot (1975).

Fig. 3 Cross sectional conceptual model illustrating the proposed modes of sedimentation in the epishelf Moutonnée Lake during periods of **(a)** ice-shelf presence and **(b)** ice-shelf absence. See text and Smith et al. (2006) for further explanation.

Fig. 4 Summary geological map of Alexander Island and western Palmer Land showing the location of Moutonnée, Ablation, and Citadel Bastion Lakes, the directional flow regime of ice within George VI Ice Shelf (Potter and Paren, 1985), superficial meltpond development and ice flow patterns of George VI Ice Shelf, and location of R stations in Palmer Land with REE, Sr and Nd isotope data (black numbered circles); Notes: AB=Ablation Lake; ML=Moutonnée Lake; CIB=Citadel Bastion Lake; Geological Terranes: WD=Western Domain; CD=Central Domain.

Fig. 5 Distribution and masses of individual clasts (line graphs) and clast shape summaries (pie charts) for ML, AB, CIB cores. Radiocarbon data are uncalibrated reported ages from *Globocassidulina* sp. apart from asterisked ages, which are from *Cibicides* sp. Ages have been rounded to the nearest 10 years with 1σ errors. See Table 1 for full list of calibrated ages and probability distributions.

Fig. 6 Individual clast composition and position of individual >8 mm clasts in the (a) ML, (b) AB and (c) CIB lake cores

Fig. 7 Summary of principal lithological composition for >8 mm clasts in the ML, AB and CIB lake cores

Fig. 8 εNd_i plot comparing new clast data and ML core <63 μm fraction data with published NW Palmer Land data from Millar et al. (2001).

Tables

Table 1 Radiocarbon dates from lake deposits on Alexander Island, Antarctic Peninsula.

Method summary: All cores were transported frozen to the UK. Cores were cut frozen and stored in the dark. Sub-samples for dating were extracted from the central portion of an undisturbed half-section of the core; Notes: a=Foraminifera radiocarbon ages (ML core only): Two species (*Globocassidulina* sp. and *Cibicides* sp.) were analysed at three AMS-dating facilities, Scottish Universities Environmental Research Centre, University of Glasgow (SUERC), Beta Analytical (BETA), University of Arizona (AA). Forams analysed at Beta Analytical received no pre-treatment. Forams analysed at SUERC and Arizona were hydrolysed to CO_2 using 85% orthophosphoric acid (AnalaR). Bulk sediment ages from ML, AB and CIB cores: CAMS/AA samples were digested in 2M HCl (80^{o}C, 10 hours) washed free of mineral acid with distilled water, dried and homogenised. Total carbon in a known weight of the pre-treated sample was recovered as CO_2 by heating with CuO in a sealed quartz tube. The gas was converted to graphite by Fe/Zn reduction. Samples were analysed at the Center for Accelerator Mass Spectrometry (CAMS), Lawrence Livermore National Laboratory, University of California and University of Arizona AMS facility (AA). BETA bulk sample was acid washed in HCl; BETA humin sample was pre-treated with hot HCl acid washes, then NaOH was used to remove secondary organic acids and the soluble fraction isolated/filtered/combined with acid and dried prior to combustion; b= AB=Ablation Lake, ML=Moutonnée Lake, CIB=Citadel Bastion Lake; c=BOC=Bulk Organic Carbon, OM=Organic Matter; *=an attempt was made to date the humic fraction of this sample, but there was insufficient carbon; d=all ages were corrected for $\delta^{13}C$ using $\delta^{13}C$ PDB (‰) ± 0.1 values: additional SUERC $\delta^{13}C$ values are measured on OPTIMA dual inlet mass spectrometer; e= Reported radiocarbon ages are ^{14}C yrs B.P. ± 1σ rounded to the nearest ten years; f=Calibrations were performed in Calib v. 4.4 (www.calib.org/calib/) (Stuvier and Reimer, 1993) with a marine reservoir correction factor that assumes forams source 100% marine carbon and ΔR=900 yr, i.e., 1300-400 year global marine reservoir offset (Berkmann and Forman, 1996; Stuvier et al., 1998); g=Percentage probability age distributions for calibrated data excluding results with a <5% probability.

Table 2 Principal clast group statistics for all cores examined (ML, AB and CIB combined data)

Notes: a=I-P=plutonic igneous clasts, I-V=Volcanic igneous clasts, S-MS=sedimentary or meta-sedimentary clasts; xl=crystal, Sst=sandstone, tuff.=tuffaceous, f-mg=fine-medium grained, m-cg=medium-coarse grained; b=Roundness scale (0-5) as defined in Pettijohn et al. (1987); c=shape classes, where P=prolate, E=equant, O=oblate, B=bladed

(Tucker, 1981). Values are statistically robust where more than 117 clasts exist (cf. Vermeesch, 2004); d=FeO is the percentage of clasts with iron staining present on the outside of the clast. All errors are 1σ.

Table 3 Summary of selected REE and isotopic data. Main clast groups discussed in text are in bold.

Notes: a=Clast isochron whole rock Rb-Sr age estimate. Palmer Land outcrop ages are independently determined age of plutonic rocks from Palmer Land (Wareham et al., 1997; Millar et al., 2001); b=εNd data as shown in Fig. 15; c=TDM is the two-stage depleted mantle model age in Ga, and represents an estimate of the time of extraction of the parental magma of each sample from a theoretical depleted mantle reservoir (Depaolo et al., 1991). Method summary: Samples were sawn in half and thin sections made from one half. The outer/weathered surfaces of the other half were removed by grinding, the remaining core crushed in a mini-rock splitter and ground by hand to a fine powder in a clean agate pestle and mortar. Powders were analysed for ten major elements using fused-disc method in a Philips PW2404 wavelength-dispersive, sequential X-ray fluorescence spectrometer following method of Norrish and Hutton (1969). The spectrometer was calibrated for major-element analysis with international standard samples (PCC1, BEN, BIR1, AGV1, RGM1, ALI, FKN), using concentrations recommended by Govindaraju (1994). Precision and accuracy are typically 5-10% for most major elements. Trace element and REE analysis was undertaken at Scottish Universities Environmental Research Centre (SUERC) following procedures in Olive et al. (2001). In summary, 0.1 g of material was dissolved by a simple tri-acids digestion (4 ml of 48 % (29 M) HF, 50 % (16 M) HNO_3 and 10 % (1 M) HCl) in a 15 ml screw cap Teflon Savillex beaker and subsequently diluted in 5% HNO_3 for analyses. Residual organic compounds present in some clast samples were removed by additional treatment with 30% H_2O_2. A VG Elemental PQ2 Plus fitted with a Meinhard nebulizer and a water-cooled glass Scott double pass spray chamber was used. Instrumental sensitivity was set up to 35 million counts per second for 1 ppm ^{115}In. Data acquisition was made in Peak Jumping mode with 3 points per peak and 3 replicates of 90 seconds each. ^{115}In, ^{102}Ru and ^{185}Re were used as internal standards. The quality of the data was controlled by regular analyses of geostandard BCR. Other geostandards (DR-N; MA-N; BEN; BCR; AGV) were also analysed to double-check the quality of the data. All data are expressed in ppm and analysed on a carbonate-free basis to avoid the influence of biogenic Ca. Uncertainties are ±1-2% (Olive et al., 2001). Rb-Sr and Sm-Nd isotope analysis was undertaken at the NERC Isotope Geosciences Laboratory following the methods of Pankhurst et al. (1993). Sr isotope compositions were determined using static multicollection on a Thermo-Finnegan Triton mass-spectrometer to an internal precision of better than 5 ppm (1 s.e.m.). During the period of analysis, 13 analyses of the Sr isotope standard NBS987 gave a value of 0.710249±0.000006 (2σ). Nd isotope compositions were determined using static multicollection on a Thermo-Finnegan Triton mass spectrometer. Sixteen analyses of the internal J&M Nd isotope standard gave a value of 0.511113±0.000004 (2σ); reported $^{143}Nd/^{144}Nd$ values were normalised to a value of 0.511130 for this standard, equivalent to 0.511864 for La

Jolla. Blanks for Sr and Nd were less than 500 pg and 180 pg respectively. The full major, trace and REE dataset is available on request.

Table 4 Summary of modes of transportation and deposition for different clast groups in the ML, AB and CIB cores.

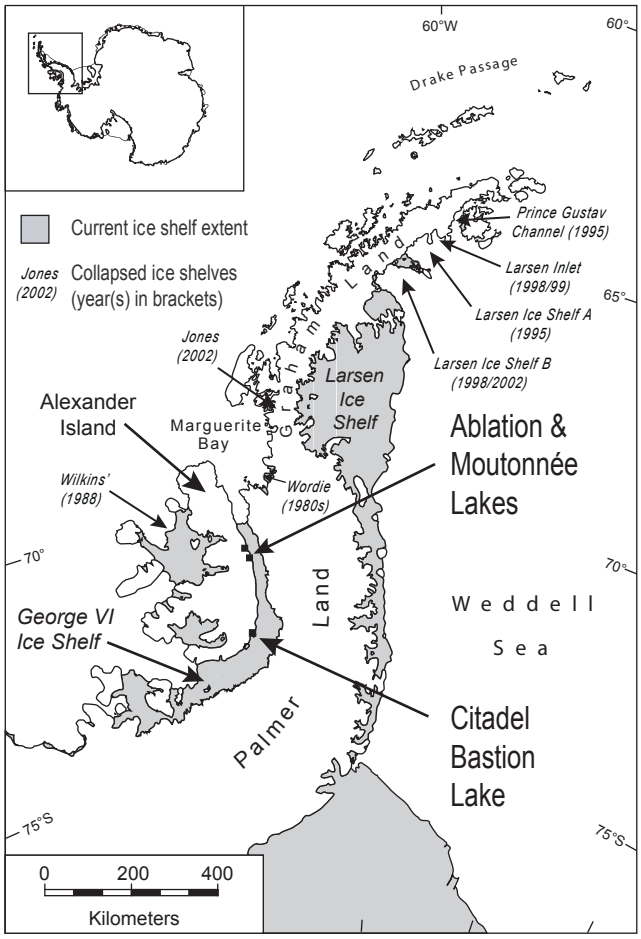
60°W
60°
Drake Passage
Current ice shelf extent
Jones (2002) Collapsed ice shelves (year(s) in brackets)
Prince Gustav Channel (1995)
Larsen Inlet (1998/99)
Larsen Ice Shelf A (1995)
Larsen Ice Shelf B (1998/2002)
65°
Jones (2002)
Larsen Ice Shelf
Alexander Island
Marguerite Bay
Wilkins' (1988)
Wordie (1980s)
Ablation & Moutonnée Lakes
70°
Graham Land
Weddell Sea
George VI Ice Shelf
Palmer Land
Citadel Bastion Lake
75°S
0 200 400
Kilometers

Fig. 1

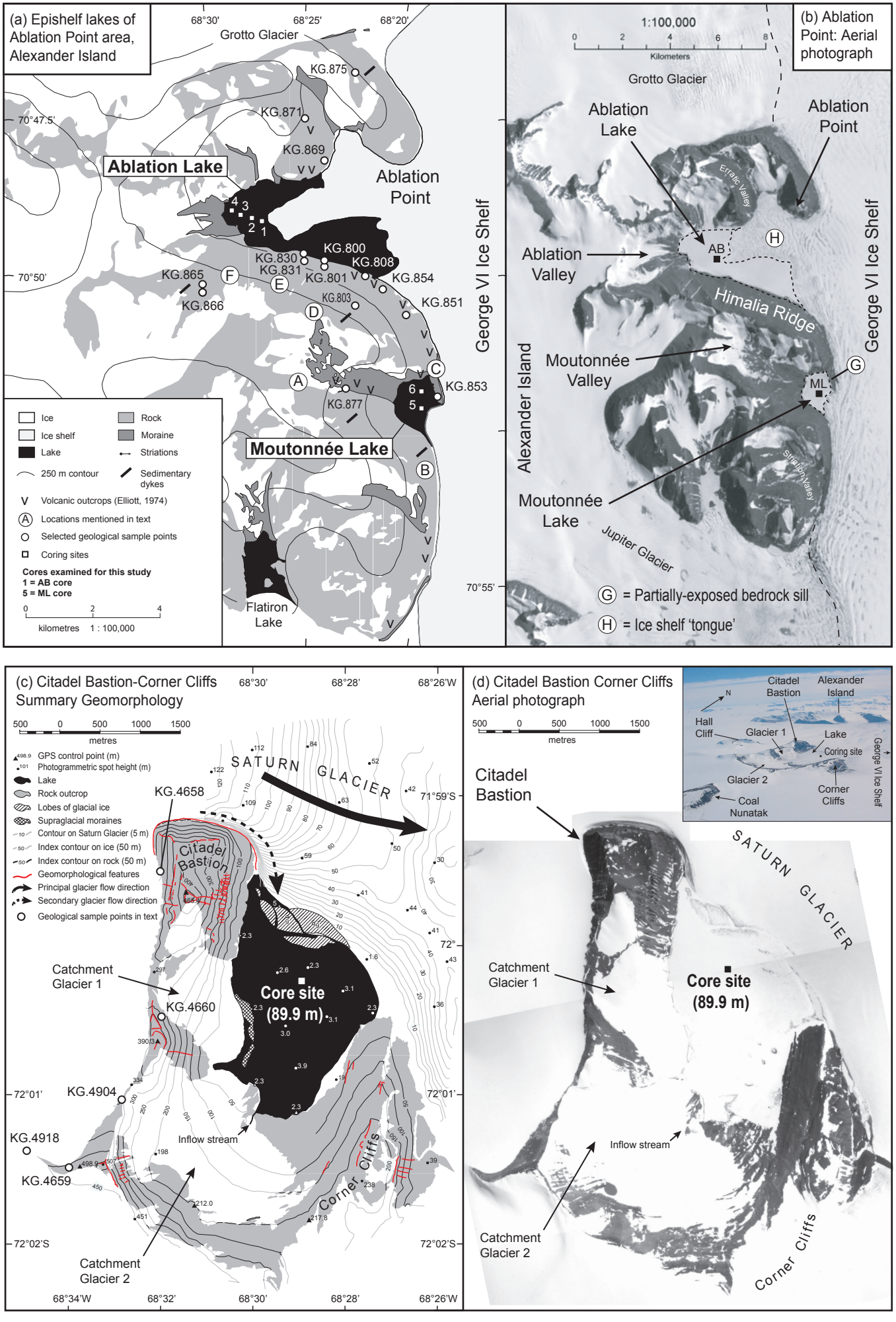
(a) Epishelf lakes of Ablation Point area, Alexander Island
68°30'
68°25'
68°20'
Grotto Glacier
KG.875
KG.871
KG.869
70°47.5'
Ablation Lake
Ablation Point
KG.800
KG.830
KG.831
KG.808
KG.801
KG.854
KG.865
KG.866
70°50'
KG.803
KG.851
George VI Ice Shelf
KG.853
KG.877
Moutonnée Lake
Flatiron Lake
70°55'
Ice
Ice shelf
Lake
Rock
Moraine
Striations
250 m contour
Sedimentary dykes
Volcanic outcrops (Elliott, 1974)
Locations mentioned in text
Selected geological sample points
Coring sites
Cores examined for this study
1 = AB core
5 = ML core
kilometres 1 : 100,000
(b) Ablation Point: Aerial photograph
1:100,000
Kilometers
Grotto Glacier
Ablation Lake
Ablation Point
Erratic Valley
Ablation Valley
AB
Himalia Ridge
Moutonnée Valley
ML
Alexander Island
Moutonnée Lake
Jupiter Glacier
G = Partially-exposed bedrock sill
H = Ice shelf 'tongue'
(c) Citadel Bastion-Corner Cliffs Summary Geomorphology
68°30'
68°28'
68°26'W
metres
GPS control point (m)
Photogrammetric spot height (m)
Lake
Rock outcrop
Lobes of glacial ice
Supraglacial moraines
Contour on Saturn Glacier (5 m)
Index contour on ice (50 m)
Index contour on rock (50 m)
Geomorphological features
Principal glacier flow direction
Secondary glacier flow direction
Geological sample points in text
SATURN GLACIER
71°59'S
KG.4658
Citadel Bastion
Catchment Glacier 1
KG.4660
Core site (89.9 m)
72°
72°01'
KG.4904
KG.4918
KG.4659
Inflow stream
Corner Cliffs
72°02'S
Catchment Glacier 2
68°34'W
68°32'
(d) Citadel Bastion Corner Cliffs Aerial photograph
Citadel Bastion
Alexander Island
Hall Cliff
Glacier 1
Lake
Coring site
Glacier 2
Corner Cliffs
Coal Nunatak
George VI Ice Shelf
SATURN GLACIER
Catchment Glacier 1
Core site (89.9 m)
Inflow stream
Catchment Glacier 2
Corner Cliffs

Fig. 2

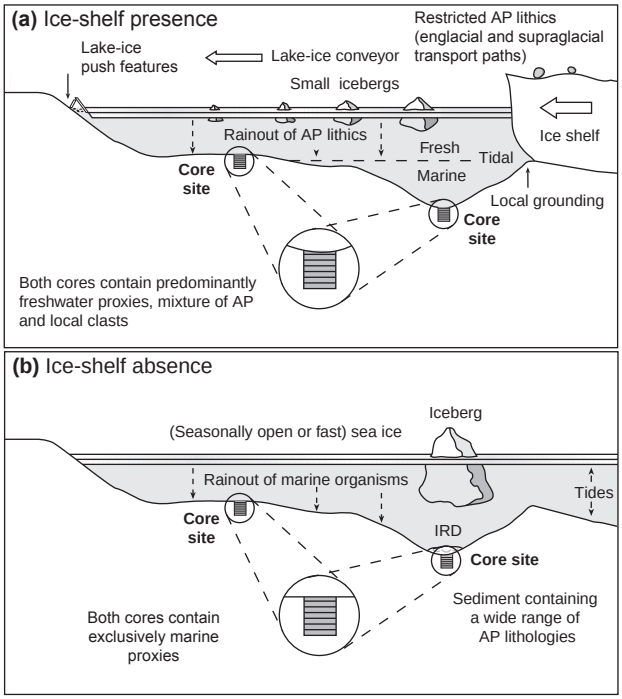
(a) Ice-shelf presence
Restricted AP lithics
(englacial and supraglacial
transport paths)
Lake-ice
push features
Lake-ice conveyor
Small icebergs
Ice shelf
Rainout of AP lithics
Fresh
Tidal
Marine
Core
site
Local grounding
Core
site
Both cores contain predominantly
freshwater proxies, mixture of AP
and local clasts
(b) Ice-shelf absence
Iceberg
(Seasonally open or fast) sea ice
Rainout of marine organisms
Tides
Core
site
IRD
Core site
Sediment containing
a wide range of
AP lithologies
Both cores contain
exclusively marine
proxies

Fig. 3

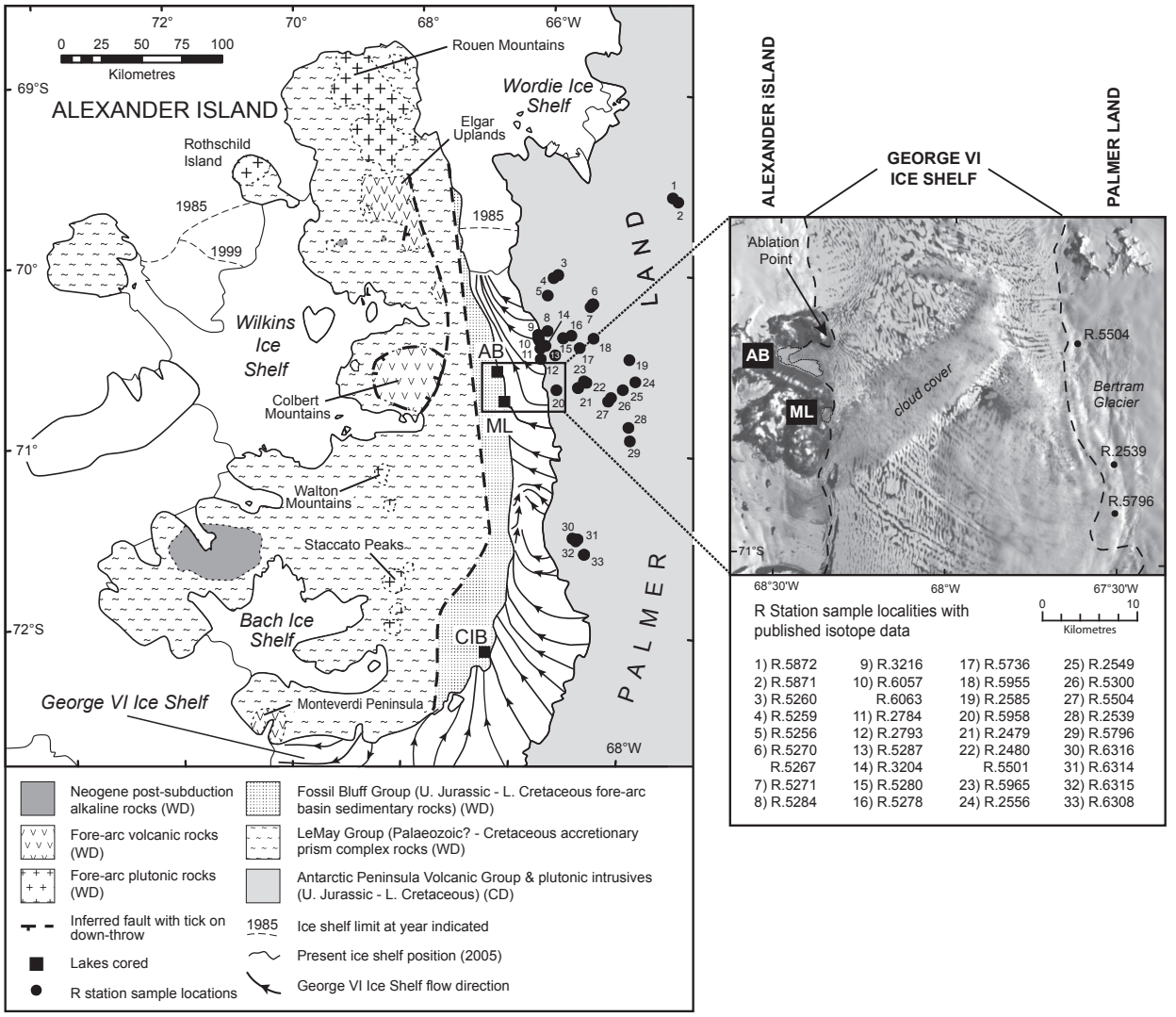
72°
70°
68°
66°W
0 25 50 75 100
Kilometres
69°S
ALEXANDER ISLAND
Rothschild Island
Rouen Mountains
Wordie Ice Shelf
Elgar Uplands
1985
1999
70°
Wilkins Ice Shelf
AB
ML
Colbert Mountains
71°
Walton Mountains
Staccato Peaks
Bach Ice Shelf
CIB
72°S
George VI Ice Shelf
Monteverdi Peninsula
PALMER LAND
68°W
Neogene post-subduction alkaline rocks (WD)
Fore-arc volcanic rocks (WD)
Fore-arc plutonic rocks (WD)
Inferred fault with tick on down-throw
Lakes cored
R station sample locations
Fossil Bluff Group (U. Jurassic - L. Cretaceous fore-arc basin sedimentary rocks) (WD)
LeMay Group (Palaeozoic? - Cretaceous accretionary prism complex rocks (WD)
Antarctic Peninsula Volcanic Group & plutonic intrusives (U. Jurassic - L. Cretaceous) (CD)
1985 Ice shelf limit at year indicated
Present ice shelf position (2005)
George VI Ice Shelf flow direction

ALEXANDER ISLAND
GEORGE VI ICE SHELF
PALMER LAND
Ablation Point
AB
ML
cloud cover
R.5504
Bertram Glacier
R.2539
R.5796
71°S
68°30'W
68°W
67°30'W
0 10
Kilometres
R Station sample localities with published isotope data
1) R.5872
2) R.5871
3) R.5260
4) R.5259
5) R.5256
6) R.5270
R.5267
7) R.5271
8) R.5284
9) R.3216
10) R.6057
R.6063
11) R.2784
12) R.2793
13) R.5287
14) R.3204
15) R.5280
16) R.5278
17) R.5736
18) R.5955
19) R.2585
20) R.5958
21) R.2479
22) R.2480
R.5501
23) R.5965
24) R.2556
25) R.2549
26) R.5300
27) R.5504
28) R.2539
29) R.5796
30) R.6316
31) R.6314
32) R.6315
33) R.6308

Fig. 4

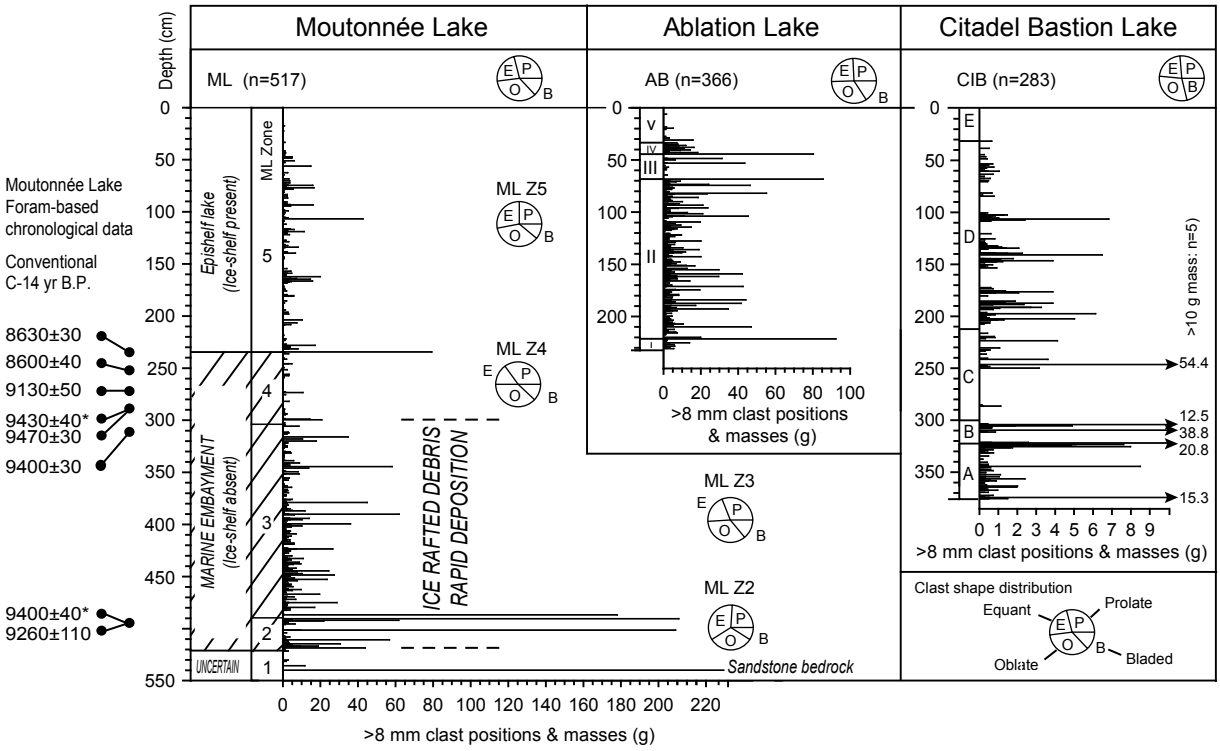
Moutonnée Lake
Ablation Lake
Citadel Bastion Lake
Depth (cm)
ML (n=517)
AB (n=366)
CIB (n=283)
Moutonnée Lake
Foram-based
chronological data
Conventional
C-14 yr B.P.
8630±30
8600±40
9130±50
9430±40*
9470±30
9400±30
9400±40*
9260±110
Epishelf lake
(Ice-shelf present)
MARINE EMBAYMENT
(Ice-shelf absent)
UNCERTAIN
ML Zone
ML Z5
ML Z4
ML Z3
ML Z2
ICE RAFTED DEBRIS
RAPID DEPOSITION
Sandstone bedrock
>8 mm clast positions & masses (g)
>10 g mass: n=5)
54.4
12.5
38.8
20.8
15.3
Clast shape distribution
Equant
Prolate
Oblate
Bladed

Fig. 5

Fig. 6

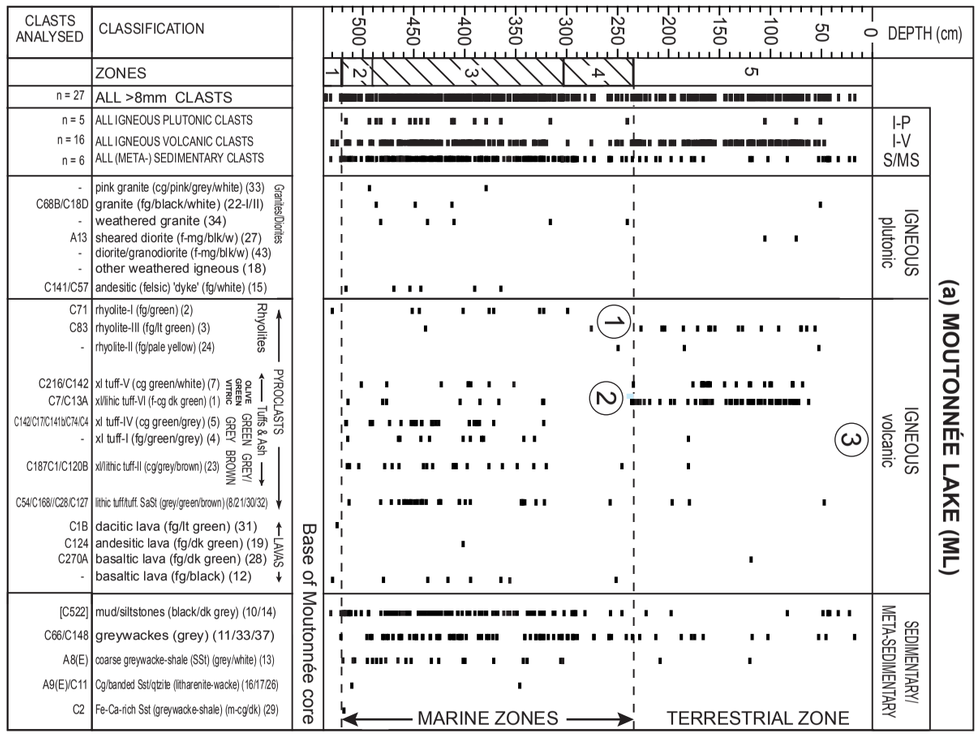
(a) MOUTONNÉE LAKE (ML)
CLASTS ANALYSED
CLASSIFICATION
ZONES
n = 27 ALL >8mm CLASTS
n = 5 ALL IGNEOUS PLUTONIC CLASTS
n = 16 ALL IGNEOUS VOLCANIC CLASTS
n = 6 ALL (META-) SEDIMENTARY CLASTS
- pink granite (cg/pink/grey/white) (33)
C68B/C18D granite (fg/black/white) (22-I/II)
- weathered granite (34)
A13 sheared diorite (f-mg/blk/w) (27)
- diorite/granodiorite (f-mg/blk/w) (43)
- other weathered igneous (18)
C141/C57 andesitic (felsic) 'dyke' (fg/white) (15)
Granites/Diorites
C71 rhyolite-I (fg/green) (2)
C83 rhyolite-III (fg/lt green) (3)
- rhyolite-II (fg/pale yellow) (24)
Rhyolites
C216/C142 xl tuff-V (cg green/white) (7)
C7/C13A xl/lithic tuff-VI (f-cg dk green) (1)
C142/C17/C141b/C74/C4 xl tuff-IV (cg green/grey) (5)
- xl tuff-I (fg/green/grey) (4)
C187C1/C120B xl/lithic tuff-II (cg/grey/brown) (23)
C54/C168//C28/C127 lithic tuff/tuff. SaSt (grey/green/brown) (8/21/30/32)
OLIVE GREEN VITRIC
GREEN GREY
GREY/ BROWN
Tuffs & Ash
PYROCLASTS
C1B dacitic lava (fg/lt green) (31)
C124 andesitic lava (fg/dk green) (19)
C270A basaltic lava (fg/dk green) (28)
- basaltic lava (fg/black) (12)
LAVAS
[C522] mud/siltstones (black/dk grey) (10/14)
C66/C148 greywackes (grey) (11/33/37)
A8(E) coarse greywacke-shale (SSt) (grey/white) (13)
A9(E)/C11 Cg/banded Sst/qtzite (litharenite-wacke) (16/17/26)
C2 Fe-Ca-rich Sst (greywacke-shale) (m-cg/dk) (29)
Base of Moutonnée core
DEPTH (cm)
500 450 400 350 300 250 200 150 100 50 0
1 2 3 4 5
I-P
I-V
S/MS
IGNEOUS plutonic
IGNEOUS volcanic
SEDIMENTARY/ META-SEDIMENTARY
MARINE ZONES
TERRESTRIAL ZONE

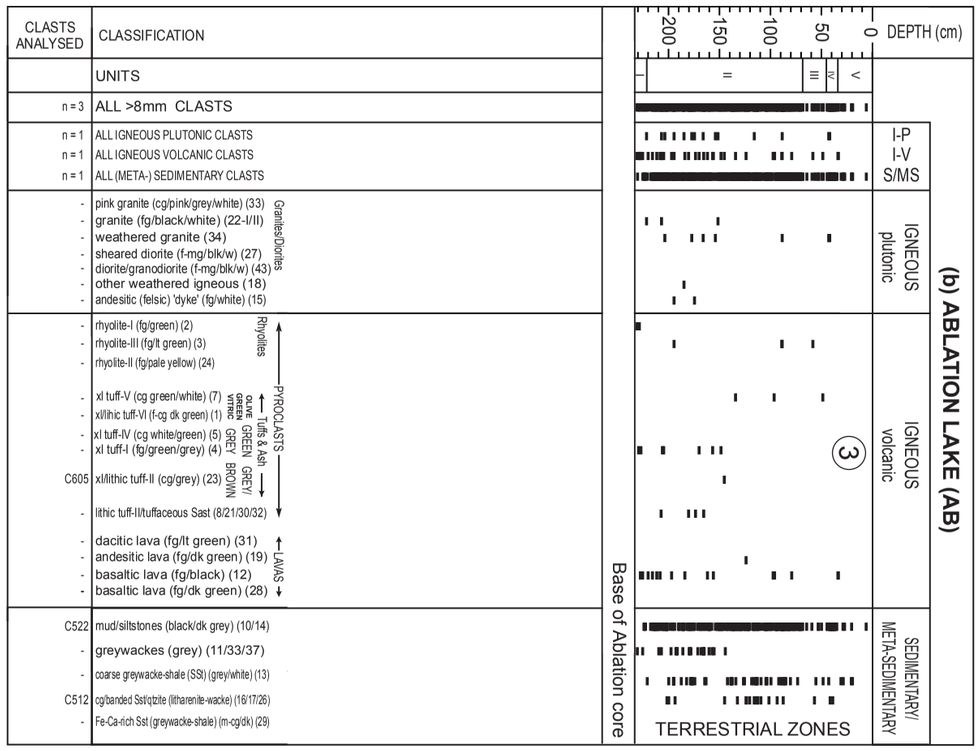
(b) ABLATION LAKE (AB)
CLASTS ANALYSED
CLASSIFICATION
UNITS
n = 3 ALL >8mm CLASTS
n = 1 ALL IGNEOUS PLUTONIC CLASTS
n = 1 ALL IGNEOUS VOLCANIC CLASTS
n = 1 ALL (META-) SEDIMENTARY CLASTS
- pink granite (cg/pink/grey/white) (33)
- granite (fg/black/white) (22-I/II)
- weathered granite (34)
- sheared diorite (f-mg/blk/w) (27)
- diorite/granodiorite (f-mg/blk/w) (43)
- other weathered igneous (18)
- andesitic (felsic) 'dyke' (fg/white) (15)
Granites/Diorites
- rhyolite-I (fg/green) (2)
- rhyolite-III (fg/lt green) (3)
- rhyolite-II (fg/pale yellow) (24)
Rhyolites
- xl tuff-V (cg green/white) (7)
- xl/lithic tuff-VI (f-cg dk green) (1)
- xl tuff-IV (cg white/green) (5)
- xl tuff-I (fg/green/grey) (4)
C605 xl/lithic tuff-II (cg/grey) (23)
OLIVE GREEN VITRIC
GREEN GREY
GREY/ BROWN
Tuffs & Ash
PYROCLASTS
- lithic tuff-II/tuffaceous Sast (8/21/30/32)
- dacitic lava (fg/lt green) (31)
- andesitic lava (fg/dk green) (19)
- basaltic lava (fg/black) (12)
- basaltic lava (fg/dk green) (28)
LAVAS
C522 mud/siltstones (black/dk grey) (10/14)
- greywackes (grey) (11/33/37)
- coarse greywacke-shale (SSt) (grey/white) (13)
C512 cg/banded Sst/qtzite (litharenite-wacke) (16/17/26)
- Fe-Ca-rich Sst (greywacke-shale) (m-cg/dk) (29)
Base of Ablation core
DEPTH (cm)
200 150 100 50 0
I II III IV V
I-P
I-V
S/MS
IGNEOUS plutonic
IGNEOUS volcanic
SEDIMENTARY/ META-SEDIMENTARY
TERRESTRIAL ZONES

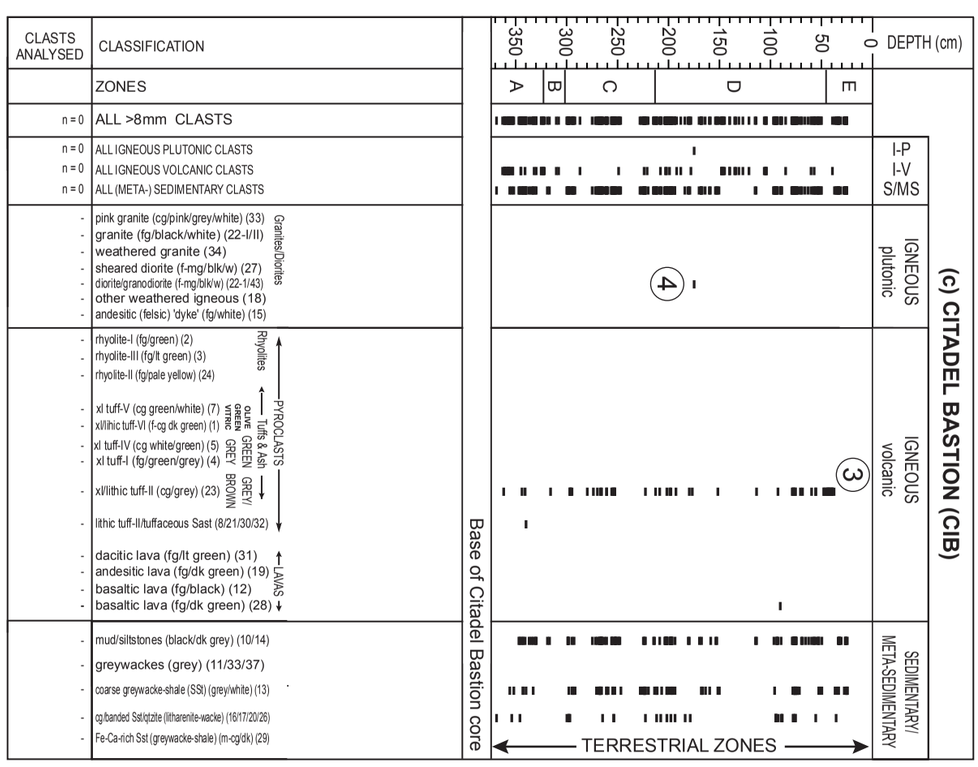
(c) CITADEL BASTION (CIB)
CLASTS ANALYSED
CLASSIFICATION
ZONES
n = 0 ALL >8mm CLASTS
n = 0 ALL IGNEOUS PLUTONIC CLASTS
n = 0 ALL IGNEOUS VOLCANIC CLASTS
n = 0 ALL (META-) SEDIMENTARY CLASTS
- pink granite (cg/pink/grey/white) (33)
- granite (fg/black/white) (22-I/II)
- weathered granite (34)
- sheared diorite (f-mg/blk/w) (27)
- diorite/granodiorite (f-mg/blk/w) (22-1/43)
- other weathered igneous (18)
- andesitic (felsic) 'dyke' (fg/white) (15)
Granites/Diorites
- rhyolite-I (fg/green) (2)
- rhyolite-III (fg/lt green) (3)
- rhyolite-II (fg/pale yellow) (24)
Rhyolites
- xl tuff-V (cg green/white) (7)
- xl/lithic tuff-VI (f-cg dk green) (1)
- xl tuff-IV (cg white/green) (5)
- xl tuff-I (fg/green/grey) (4)
- xl/lithic tuff-II (cg/grey) (23)
OLIVE GREEN VITRIC
GREEN GREY
GREY/ BROWN
Tuffs & Ash
PYROCLASTS
- lithic tuff-II/tuffaceous Sast (8/21/30/32)
- dacitic lava (fg/lt green) (31)
- andesitic lava (fg/dk green) (19)
- basaltic lava (fg/black) (12)
- basaltic lava (fg/dk green) (28)
LAVAS
- mud/siltstones (black/dk grey) (10/14)
- greywackes (grey) (11/33/37)
- coarse greywacke-shale (SSt) (grey/white) (13)
- cg/banded Sst/qtzite (litharenite-wacke) (16/17/20/26)
- Fe-Ca-rich Sst (greywacke-shale) (m-cg/dk) (29)
Base of Citadel Bastion core
DEPTH (cm)
350 300 250 200 150 100 50 0
A B C D E
I-P
I-V
S/MS
IGNEOUS plutonic
IGNEOUS volcanic
SEDIMENTARY/ META-SEDIMENTARY
TERRESTRIAL ZONES

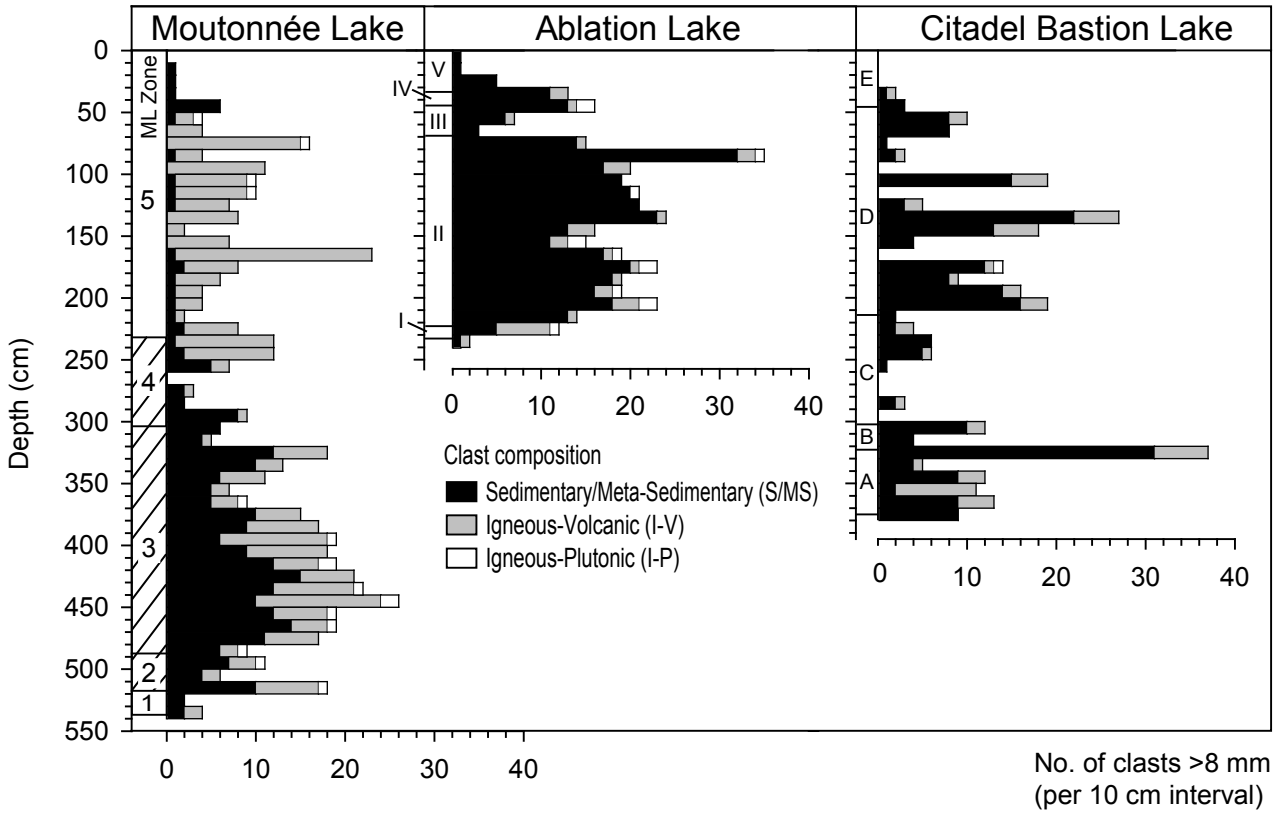
Moutonnée Lake
Ablation Lake
Citadel Bastion Lake
Depth (cm)
ML Zone
1
2
3
4
5
I
II
III
IV
V
A
B
C
D
E
Clast composition
Sedimentary/Meta-Sedimentary (S/MS)
Igneous-Volcanic (I-V)
Igneous-Plutonic (I-P)
No. of clasts >8 mm
(per 10 cm interval)

Fig. 7

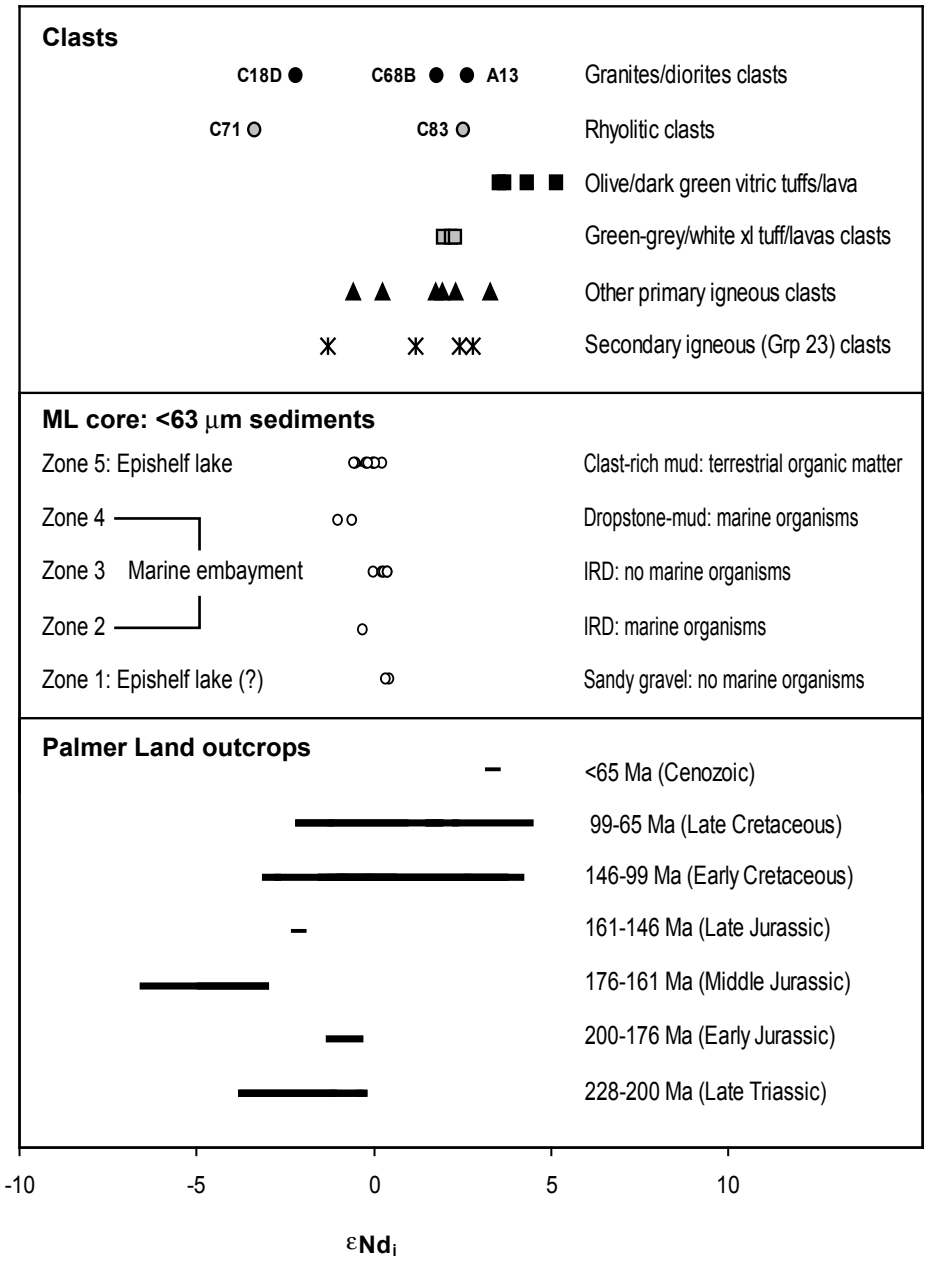
Clasts
C18D
C68B
A13
Granites/diorites clasts
C71
C83
Rhyolitic clasts
Olive/dark green vitric tuffs/lava
Green-grey/white xl tuff/lavas clasts
Other primary igneous clasts
Secondary igneous (Grp 23) clasts
ML core: <63 μm sediments
Zone 5: Epishelf lake
Clast-rich mud: terrestrial organic matter
Zone 4
Dropstone-mud: marine organisms
Zone 3
Marine embayment
IRD: no marine organisms
Zone 2
IRD: marine organisms
Zone 1: Epishelf lake (?)
Sandy gravel: no marine organisms
Palmer Land outcrops
<65 Ma (Cenozoic)
99-65 Ma (Late Cretaceous)
146-99 Ma (Early Cretaceous)
161-146 Ma (Late Jurassic)
176-161 Ma (Middle Jurassic)
200-176 Ma (Early Jurassic)
228-200 Ma (Late Triassic)
-10
-5
0
5
10
εNdi

Fig. 8

Laboratory[a] Code	Sample ID (Depth)[b]	Dated foram[c] species or fraction	Lithology	$\delta^{13}C_{PDB}$ (‰ ± 0.1)	$\delta^{13}C_{AMS}$[d] (‰ ± 0.1)	^{14}C enrichment (% Modern ± 1σ)	^{14}C age[e] (^{14}C yr B.P.)	Calibrated 2σ age range[f] (cal yr B.P.)	Prob.[g] (%)	Median age (cal yr B.P.)
(i) Foraminifera ages (ML core only)										
SUERC-575	ML2A (243-246 cm)	*Globocassidulina* sp.	Silty clay	0.6	3.3	34.14 ± 0.13	8630 ± 30	7967 - 8372	100	8188
SUERC-576	ML2A (252-255 cm)	*Globocassidulina* sp.	Silty clay	1.0	3.7	34.27 ± 0.15	8600 ± 40	7945 - 8355	100	8155
SUERC-577	ML2A (270-272 cm)	*Globocassidulina* sp.	Silty clay	0.2	1.7	32.11 ± 0.19	9130 ± 50	8451 - 8941	100	8712
SUERC-578	ML2A (280-281cm)	*Globocassidulina* sp.	Silty clay	0.5	4.8	30.78 ± 0.11	9470 ± 30	8830 - 9434	98	9055
BETA-177300	ML2A (280-281 cm)	*Cibicides* sp.	Silty clay	-0.7	-	30.90 ± 0.20	9430 ± 40	8801 - 9425	99	9014
SUERC-579	ML2A (291-293 cm)	*Globocassidulina* sp.	Silty clay	0.4	4.4	31.02 ± 0.13	9400 ± 30	8742 - 9136	80	8985
								9188 - 9418	19	-
AA-54874	ML4 (494-496 cm)	*Globocassidulina* sp.	Silty clay	0.6	n/a	31.58 ± 0.44	9260 ± 110	8445 - 9084	96	8827
BETA-177301	ML4 (494-495 cm)	*Cibicides* sp.	Silty clay	-0.3	n/a	31.00 ± 0.20	9400 ± 40	8730 - 9138	79	8983
								9186 - 9419	20	-
(ii) Surface ages										
CAMS-78992	ML surface sediment	BOC	Silty clay	-25.9	n/a	15.3 ± 0.1	15100 ± 50	Unreliable age – not calibrated		
AA-54875	ML1A (3-10 cm)	OM	n/a	-30.3	n/a	8.6 ± 0.2	19720 ± 160	Unreliable age – not calibrated		
CAMS-78994	AB Surface	BOC	Silty clay	-24.7	n/a	17.1 ± 0.1	14180 ± 50	Unreliable age – not calibrated		
BETA-174765	CIB (0-4 cm)	BOC	Clay	-24.8	n/a	12.0 ± 0.1	17000 ± 70	Unreliable age – not calibrated		
BETA-175625	CIB (0-4 cm)	Humin*	n/a	-24.4	n/a	7.6 ± 0.1	20720 ± 100	Unreliable age – not calibrated		
(iii) CIB bulk 'organic-rich' sediment peak samples										
BETA-194316	CIB-P1 (20-22 cm)	BOC	Clay	-24.4	n/a	17.9 ± 0.1	13800 ± 60	Unreliable age – not calibrated		
BETA-194315	CIB-P5 (161-163 cm)	BOC	Clay	-25.0	n/a	6.3 ± 0.1	22270 ± 100	Unreliable age – not calibrated		
BETA-194314	CIB-P7 (274-276 cm)	BOC	Clay	-26.4	n/a	3.5 ± 0.1	26900 ± 160	Unreliable age – not calibrated		

Table 1

Rock type		Class[a]	Group summary description	Groups	No. of Clasts (n)	Mean Clast Mass (g)	Mean[b] Roundness	Shape Class[c] P-E-O-B (%)	Striated Clasts (%)	FeO[d] (%)
PRIMARY IGNEOUS										
(i)	Granites	I-P	Fresh granites	22-I/II/33	8	41.2±22.3	1.6±0.5	38-13-50-0	0	38
		I-P	Weathered granites	34	11	5.08±1.99	2.1±0.3	18-27-45-9	9	27
	Granodiorite/diorite	I-P	Foliated & unaltered	27/43	4	7.07±3.21	1.5±0.6	25-25-50-0	0	25
(ii)	Rhyolites	I-V	Green Rhyolite	2	11	5.69±2.26	2.9±0.5	27-45-18-9	9	18
		I-V	Light green Rhyolite	3	21	3.21±0.81	1.7±0.3	10-35-40-15	0	10
(iii)	Crystal/lithic Tuffs	I-V	Olive/dark green vitric xl tuff	1/7	124	5.69±1.82	1.2±0.1	25-28-36-12	1	8
		I-V	Grey-green/white xl/lithic tuff	4/5	49	3.92±1.30	1.9±0.1	27-33-33-8	0	6
(iv)	Other Primary Igneous	I-P	Andesitic/felsic dyke	15	8	12.1±7.2	2.1±0.4	0-25-63-13	0	0
		I-V	Basaltic black lava	12	23	10.8±2.6	1.7±0.3	27-14-41-18	36	14
SECONDARY IGNEOUS										
(v)	Grp. 23 lithic Tuffs/tuff. Sst	I-V	Grey-white lithic tuff/tuff. Sst	23	78	1.76±0.31	2.1±0.1	26-26-30-18	5	5
(vi)	Other lithic Tuffs/tuff. Sst	I-V	Brown Tuffs/tuff. Sst	8/21/30/32	37	6.16±1.81	1.9±0.2	30-22-38-11	3	11
NON-IGNEOUS CLASTS										
(vii)	Sedimentary/Meta-sedimentary	S-MS	Mudstones/siltstones	10/14	467	3.73±0.39	2.5±0.1	27-20-32-21	33	11
		S-MS	Greywacke Sst (f-mg)	11/13/20	249	4.43±0.93	2.4±0.1	31-21-35-13	7	12
		S-MS	Litharenite/Greywacke Sst (m-cg)	16/17/26	50	8.23±4.79	2.6±0.1	30-32-26-12	4	14
ALL CLASTS (includes data from groups with <4 clasts)				ALL	1166	4.83±0.44	2.22±0.03	27-23-33-16	17	11

Table 2

Clast	Class	Classification	Group	Core	Depth (cm)	Eu/Eu*	La/Yb_N	La/Sm_N	Gd/Yb_N	Rb/Sr	$^{87}Rb/^{86}Sr$	$^{87}Sr/^{86}Sr$	Age[a] (Ma)	Sm (ppm)	Nd (ppm)	$^{147}Sm/^{144}Nd$	$^{143}Nd/^{144}Nd$	$^{87}Sr/^{86}Sr_i$	εNd[b]	TDM[c] (Ga)
PRIMARY IGNEOUS CLASTS																				
(i) Granites/diorites																				
C68B	I-P	Hornblende Granite	22-I	ML3B	447-451	0.92	6.15	2.91	1.59	0.215	0.6222	0.706282	140	5.06	24.72	0.123779	0.512663	0.705044	1.79	0.81
C18D	I-P	Granite	22-II	ML4	483-491	0.20	5.21	3.58	1.02	0.129	0.3726	0.708066	180	5.38	27.21	0.119569	0.512435	0.707112	-2.19	1.17
A13	I-P	Sheared/foliated Diorite	27	ML1A	74-75.5	0.90	1.88	1.14	1.39	0.018	0.0507	0.704376	140	5.07	18.67	0.164286	0.512745	0.704275	2.66	0.73
(ii) Rhyolites																				
C71	I-V	Type I green Rhyolite	2	ML3B	443-446	0.72	10.76	4.33	1.50	0.738	2.1367	0.712581	180	4.32	24.35	0.107236	0.512360	0.707113	-3.37	1.26
C83	I-V	Type III lt green Rhyolite	3	ML3B	438-439	0.62	5.35	3.40	1.08	0.398	1.1525	0.707204	140	3.24	16.02	0.122363	0.512699	0.704911	2.52	0.74
(iii) Olive/dark green vitric xl Tuffs/Lavas																				
C7	I-V	Bas.-Trachyandesitic olive green xl Tuff	1	ML4	513-516	0.93	3.29	1.90	1.39	0.403	-	-	-	4.13	16.72	0.149420	0.512707	0.706785	-	-
C13A	I-V	Bas.-Trachyandesitic olive green xl Tuff	1	ML4	442-444	0.93	2.40	1.21	1.58	0.050	0.1439	0.705250	140	4.67	17.26	0.163679	0.512797	0.704964	3.69	0.63
C216	I-V	Basalt olive green/white xl Tuff	7	ML2A	233-236	1.10	4.08	2.22	1.52	0.033	0.0948	0.705281	140	3.45	13.69	0.152392	0.512779	0.705092	3.54	0.65
C142	I-V	Trachyandesitic dk green xl Tuff	7a	ML3A	386-388	0.90	2.36	1.46	1.33	0.165	0.4775	0.705812	140	5.71	22.33	0.154703	0.512865	0.704862	5.18	0.48
C124	I-V	Trachyandesitic dk green Lava	19	ML3A	400-403	0.93	2.08	1.57	1.18	1.046	3.0264	0.709626	120	4.14	15.13	0.165392	0.512835	0.704465	4.32	0.56
C270A	I-V	Basalt dk green vitric Lava	28	ML1B	118-120	1.16	2.57	1.66	1.30	0.06	-	-	-	2.26	8.464	0.161162	0.512812	0.705401	-	-
(iv) Green-grey/white xl Tuffs																				
C4	I-V	And.-trachandesitic grey-white xl/lithic Tuff	5	ML4	516-518	0.78	3.07	1.86	1.27	0.162	0.0452	0.705605	140	3.87	15.80	0.148071	0.512695	0.705515	1.98	0.79
C74	I-V	Andesitic grey-white xl/lithic Tuff	5	ML3B	441-443	1.04	5.67	3.68	1.14	0.070	0.2034	0.705541	140	2.59	13.28	0.117763	0.512679	0.705136	2.21	0.77
C141B	I-V	Andesitic grey-white/green xl/lithic Tuff	5-5a	ML3A	390-392	0.90	2.84	1.70	1.31	0.086	0.2495	0.705685	140	-	21.38	-	0.512709	0.705188	-	-
C17	I-V	Andesitic green-white xl Tuff	5a	ML4	490-494	1.34	5.76	3.23	1.31	0.031	0.0902	0.705409	140	2.00	10.16	0.119306	0.512686	0.705229	2.32	0.76
(v) Other igneous clasts																				
C1b	I-V	Dacitic Lava	31	ML4E	524-527	0.91	3.57	2.51	1.12	3.300	0.6692	0.706269	140	2.72	11.02	0.149236	0.512684	0.704937	1.74	0.81
C168	I-V	Andesite/Tuff-tuff. Sst	8a	ML2B	344-345	0.89	3.01	1.64	1.46	0.108	0.3125	0.708019	140	4.16	15.98	0.157496	0.512771	0.707397	3.3	0.67
C188	I-V	Andesitic Ashstone	36	ML2B	314-318	0.72	4.92	2.37	1.52	0.220	0.6378	0.707104	140	4.32	24.35	0.107236	0.512360	0.705835	-0.59	1.01
C141	I-P	Andesitic dyke material	15	ML3B	389-392	0.81	5.51	2.68	1.53	0.032	0.0921	0.705714	140	4.80	21.42	0.135509	0.512595	0.705531	0.25	0.94
C57	I-P	Andesitic dyke material	15	ML3B	453-455	0.91	4.73	2.17	1.63	0.032	0.0915	0.705765	140	4.18	18.63	0.135566	0.512682	0.705583	1.95	0.79
SECONDARY IGNEOUS CLASTS																				
(vi) Group 23 lithic tuff/tuffaceous Sandstones																				
C118	I-V	Grey-white lithic Tuff/Tuff. Sst	23	ML3A	411-412	0.76	3.17	1.39	1.77	0.033	0.0959	0.705483	140	4.68	18.93	0.149344	0.512655	0.705292	1.17	0.86
C120B	I-V	Grey-white lithic Tuff/Tuff. Sst	23	ML3A	408-410	0.89	6.98	2.95	1.76	0.070	0.2025	0.705727	140	4.76	21.18	0.135900	0.512726	0.705324	2.8	0.71
C187	I-V	Grey-white lithic Tuff/Tuff. Sst	23	ML2B	319-321	0.97	6.38	4.01	1.19	0.041	0.1176	0.705822	140	2.99	15.01	0.120293	0.512693	0.705588	2.44	0.75
C1	I-V	Grey-white lithic Tuff/Tuff. Sst	23	ML4	516-518	0.74	2.29	1.38	1.44	0.081	0.2342	0.705671	120	5.16	18.66	0.167115	0.512847	0.705272	4.53	0.53
C605	I-V	Grey-white lithic Tuff/Tuff. Sst	23a	AB2B	145-146	0.74	13.41	4.90	1.65	0.400	1.1575	0.708176	140	3.52	19.64	0.108204	0.512491	0.705873	-1.29	1.07
(vii) Other Tuffs/tuffaceous Sandstones																				
C127	I-V	Brown lithic Tuff	30	ML3A	398-401	0.93	3.29	1.73	1.44	0.177	0.5112	0.706063	140	4.66	18.64	0.151144	0.512753	0.705046	3.05	0.69
C28	I-V	Brown lithic Tuff	32	ML3A	400-403	0.96	3.18	1.83	1.34	0.034	0.0988	0.705721	140	3.32	13.56	0.148075	0.512668	0.705524	1.5	0.84
C54	I-V	Brown tuff. Sst	8	ML3B	452-454	0.85	2.92	1.87	1.21	0.195	0.5645	0.706187	140	4.06	16.61	0.147721	0.512697	0.705064	2.02	0.79
NON-IGNEOUS CLASTS																				
(viii) Sedimentary/Meta-sedimentary																				
C522	S-MS	Mudstone/Siltstone	14	AB2B	209-212	0.71	7.73	2.80	1.79	0.127	0.3665	0.706950	140	4.12	20.31	0.122718	0.512521	0.706221	-0.96	1.04
C66	S-MS	Greywacke-shale Sst/Agg.	11	ML3B	446-449	0.90	4.16	2.29	1.36	0.216	0.6259	0.706205	140	3.47	14.78	0.142028	0.512721	0.704959	2.59	0.73
C148	S-MS	Greywacke-shale Sst/Agg.	11	ML3A	377-382	0.87	3.48	2.13	1.29	0.083	0.2399	0.705837	140	4.40	18.07	0.147213	0.512750	0.705360	3.07	0.69
A8	S-MS	Greywacke-shale Sst	13	ML3BE	486-495	0.61	3.96	2.66	1.09	0.086	0.2476	0.705983	140	5.58	24.93	0.135412	0.512745	0.705490	3.18	0.68
A9	S-MS	Greywacke-shale Sst	16	ML4E	527-533	0.60	2.71	1.61	1.28	0.040	0.1148	0.705614	140	2.73	10.45	0.157650	0.512682	0.705386	1.55	0.83
C11	S-MS	Litharenite-wacke Sandstone/quartzite	26	ML4	510-512	0.72	5.94	2.77	1.52	0.268	0.7760	0.707584	140	3.51	16.24	0.130804	0.512585	0.706040	0.14	0.95
C512	S-MS	Mottled Sandstone	16a	AB2B	221-222	0.84	8.37	3.47	1.58	0.202	0.5842	0.707531	140	3.95	19.83	0.120367	0.512552	0.706368	-0.32	0.99
C2	S-MS	Fe-Ca-rich Greywacke-shale Sandstone	29	ML4	517-520	0.99	4.48	2.45	1.41	0.092	0.2661	0.705756	140	3.75	15.81	0.143334	0.512776	0.705227	3.64	0.64

Table 3

Mode	Predominant depositional mode (Original source-locality)	Description of clast erosion/transport/deposition process	Clast types	Clast Group example (Clast)	Cores
Local sources					
I	Erosion of Fossil Bluff Group (Alexander Island)	Clasts eroded directly from sedimentary outcrops of the Fossil Bluff Group and catchment moraines by local glacial activity and/or as dump deposits during lake ice break up events.	Most sedimentary & meta-sedimentary	14 (C522)	ML AB CIB
II	Volcanic aerial deposition (Palmer Land-Alex.Island)	Volcanic airfall deposits from Palmer Land incorporated into the Fossil Bluff Group during its formation. Clasts subsequently eroded into the lakes by local glacial activity.	Tuffs & ash	1/7 (C13A/C216)	ML AB
III	Glacial deposition (Palmer Land-Alex. Island)	Clast types originally from Palmer Land transported to Alexander Island by pre-Holocene glacial activity. Subsequently eroded by local glacial activity directly into the lake or into the lake after being incorporated into catchment moraines.	Well-rounded/ weathered granites	AB granite clast not analysed	ML AB (CIB?)
IV	Post-formation glacial (Palmer Land-Alex. Island)	Rock types originally from Palmer Land transported to Alexander Island by pre-Holocene glacial activity. Deposited in moraines or onto valley floor and subsequently eroded into the lake by local glacial activity.	Granites	22 (C68B?)	ML AB
Exotic sources					
V	Ice rafting (Palmer Land-Alex. Island)	Rock types from Palmer Land incorporated into GVIIS. Deposited as IRD from icebergs formed when GVIIS collapses. Icebergs are able to drift into newly formed marine embayments.	Wide variety of angular / coevally deposited igneous clasts	Numerous possibilities (see Zone 3 Fig. 6a)	ML
VI	Ice shelf transportation (Palmer Land-Alex. Island)	Rock types from Palmer Land transported through GVIIS and deposited in and around the lake, possibly by lake ice conveyor	Foliated / sheared diorite?	27 (A13)	ML AB?

Table 4